*Journal of Structural Geology*, Vol. 4, No. 3, pp. 313 to 342, 1982
Printed in Great Britain

0191-8141/82/030313-30 $03.00/0


# Characteristics and mode of emplacement of gneiss domes and plutonic domes in central-eastern Pyrenees*

JEAN-CLAUDE SOULA

Laboratoire de Géologie-Petrologie et Tectonophysique, Université Paul Sabatier, 38, rue des Trente Six Ponts, 31400 Toulouse France

(*Received* 23 *October* 1980; *accepted in revised form* 23 *April* 1982)

**Abstract**—Gneiss domes and plutonic granitoid domes make up almost 50% of the pre-Hercynian terrains in the Central and Eastern Pyrenees. From a structural study of the shape and internal structure of the domes and of their relationships with the enclosing rocks, it can be shown that both types of domes were emplaced diapirically during the major regional deformation phase and the peak of regional metamorphism.

The study also shows that the internal structure, the overall shape and general behaviour relative to the host rocks are similar for plutonic domes and for gneiss domes. This appears to be in good agreement with H. Ramberg's (1967, *Gravity Deformation and the Earth's Crust*. Academic Press, London; 1970, Model studies in relation to intrusion of plutonic bodies. In: *Mechanisms of Igneous Intrusion* (edited by Newall, G. & Rast, N.) *Geol. J. Spec. Issue* **2**, 261–286.) model studies showing that dome or mushroom-like structures, similar to those observed, develop when there is a small viscosity ratio between the rising body and its enclosing medium.

This implies a high crystal content for the granitoid magma. This crystal content has been estimated by (i) calculating the viscosity and density in natural conditions from petrological data for the magma considered as a suspension, using the model and program of J. P. Carron *et al.* (1978 *Bull Soc. géol. Fr.* **20**, 739–744.); (ii) using the recent results of experimental deformation of partially melted granites of I. van der Molen & M. S. Paterson (1979, *Contr. Miner. Petrol.* **70**, 299–318.) and (ii) comparing the preceding results with the data obtained by deformation experiments on rocks similar to those enclosing the domes. The minimum crystal content for the development of a dome-like structure has been, thus, estimated to about 70%, i.e. a value very close to that estimated by van der Molen & Paterson (1979) to be the critical value separating the granular framework flow from suspension-like behaviour.

The effect of small variations in the viscosity of the rising body are then simulated by centrifuge experiments. These small variations appear to exert a strong control on the shape and rate of rise of the domes. They are thought to be sufficient to account for the variations in shape and structure and the level of emplacement of the different types of gneissic and plutonic domes.

Finally, more complex experiments, with models built in order to simulate as closely as possible the natural structural evolution of the region as deduced from petrological and structural data, are reported. Their implications for the regional interpretation of the relationships between gneissic and plutonic domes is then discussed.

## INTRODUCTION

GNEISS domes, plutonic and metamorphic domes are amongst the most striking structural features in the Hercynian Pyrenees. However, their development has been little considered, and in general is taken to be a late and minor structural event independent of the major structural, metamorphic and plutonic events.

This study, on the contrary, emphasizes the major importance of dome development as a primary process controlling the structural evolution of the Pyrenees in Hercynian time. The process will be interpreted as being directly linked to, and governing the emplacement of plutonic rocks and the type of metamorphism. The study refers, essentially, to the well-exposed eastern part of the Central Pyrenees, in the Ariege Departement and neighbouring areas.

*Presented at a conference on Diapirism and Gravity Tectonics organised by the Tectonic Studies Group at the University of Leeds, 25–26 March 1980.

## REGIONAL BACKGROUND

Pre-Hercynian rocks are the essential constituents of the Pyrenees. They make up almost all the outcrops in the Axial Zone (Fig. 1) and appear as large horst-like structures within the Alpine cover to the North where they constitute the North Pyrenean Massifs.

The stratigraphy of the Upper Palaeozoic is well known (see synthesis in Mirouse 1977). It consists mainly of limestones, quartz–phyllitic pelites or sandstones and phyllitic limestones. The stratigraphy of the pre-Silurian is much less well known. Reliable fossils have been found only in the uppermost part, and give a Caradocian age. The pre-Silurian consists mainly of metasediments and gneisses. The metasedimentary series is made up of quartz–phyllitic rocks with some limestone beds. Its lower part is richer in plagioclase bearing sandstones, meta-amphibolites and ortho-amphibolites. Small intrusive bodies of basic rocks are common and ultrabasic rocks are occasionally observed. The metasedimentary series is often considered as 'Cambro-Ordovician' but without very convincing

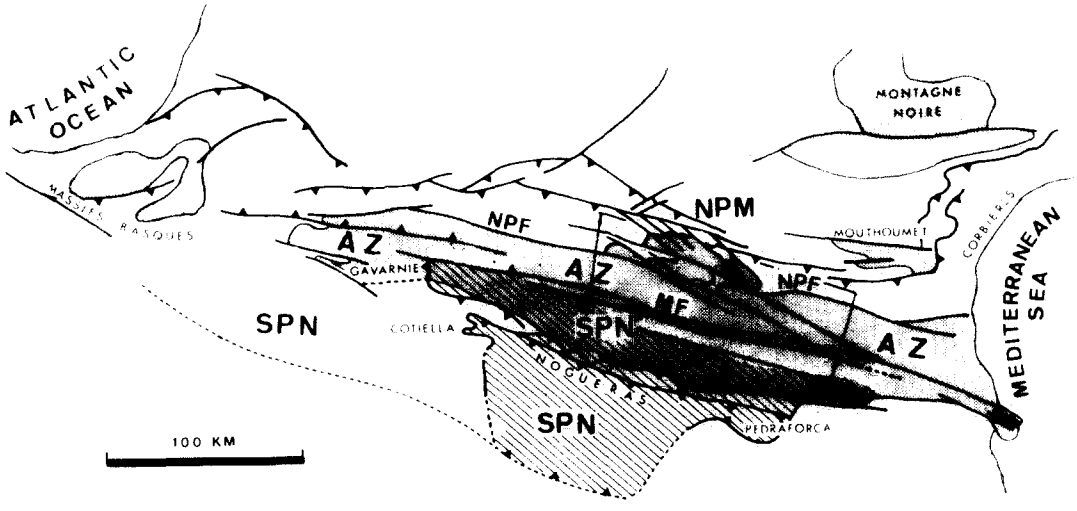


Fig. 1. Location map. Key: NPM, North Pyrenean massifs; AZ, Axial Zone; SPN, South Pyrenean Zone; NPF, North Pyrenean Fault; MF, Merens Fault.

evidence. By analogy with the nearby Montagne Noire where Precambrian metasediments have been recognized from fossil evidence in a similar metasedimentary series, it is suggested that at least the basal part of the metasedimentary series in the Pyrenees could also be Precambrian.

The gneisses are two types: granulitic gneisses, which consist of heterogeneous paragneisses and orthogneisses, and homogeneous augen-orthogneisses.

Granulitic gneisses occur beneath the metasedimentary series and are interpreted as a Precambrian basement (e.g. Zwart 1953, Lelubre 1964, Autran *et al.* 1966, Guitard 1970, Guchereau 1975, Roux 1977).

Augen-orthogneisses occur as smaller or larger massifs alternating with/or intruded within metasediments. They have also been considered by some authors to represent the Precambrian basement, originally underlying the metasedimentary series, and their occurrence within the metasediments to be due to basement-cored fold nappes (e.g. Guitard 1970). Alternatively they have been considered to be intrusive granitoids of Ordovician age (Jaeger & Zwart 1968). It should be noticed that radiometric dating of these augen gneisses has given ages of 570–535 Ma, that is Early Cambrian (Vitrac & Allègre 1971) and 475 Ma, that is Ordovician (Jaeger & Zwart 1968). The interpretation that the augen gneisses are cores of large recumbent folds is not acceptable in the studied region. Here the augen gneisses are unevenly developed and may be absent in some areas. They occur at various levels and even at rather high structural levels (see Figs. 2, 3, 8, 11 and 12) and are interpreted as intrusive sills, lenses or massifs, in agreement with Zwart (1979). However, if the lower part of the metasedimentary series where the gneisses are intruded is Precambrian, and not Cambro-Ordovician, the age of the intrusion may have been Precambrian as well as Ordovician. The hypothesis of a Precambrian intrusion has been proposed in the Western Montagne Noire where similar gneisses are clearly intrusive within the Precambrian metasediments (Debat *et al.* 1975).

Pre-Silurian and some Upper Palaeozoic rocks have been affected by Hercynian metamorphism, characterized by a very steep metamorphic gradient (up to 150° $km^{-1}$ according to Zwart 1962), grading up to produce widespread anatexis. This metamorphism appears as metamorphic domes several kilometres in extent. Contact metamorphism around plutonic massifs has similar characteristics to the regional metamorphism, indicating similar conditions. Regional metamorphic and contact metamorphic isograds may be in continuity (Soula 1970, Castaing *et al.* 1973, Barrouquère *et al.* 1976).

## REGIONAL DEFORMATION AND METAMORPHISM

In the last 15 years, the deformation history of the Hycernian Pyrenees has given rise to many controversies and several rival schemes have been proposed (e.g. Guitard 1970, 1976, 1977, Zwart 1965, 1968, 1979, Seguret & Proust 1968 a, b).

The sequence as presented here is based on investigations carried out for more than ten years by the author and other researchers from the Laboratoire de Géologie-Pétrologie of the University of Toulouse and modifies notably the preceding schemes.

Four principal Hercynian deformations have been recognized.

### *Deformation* D1

The first deformation, *D*1, was responsible for recumbent folds, *F*1, developed only locally and unevenly distributed. They are variably oriented and their amplitude ranges from several centimetres to tens of metres and locally hundreds of metres (Déramond 1971,

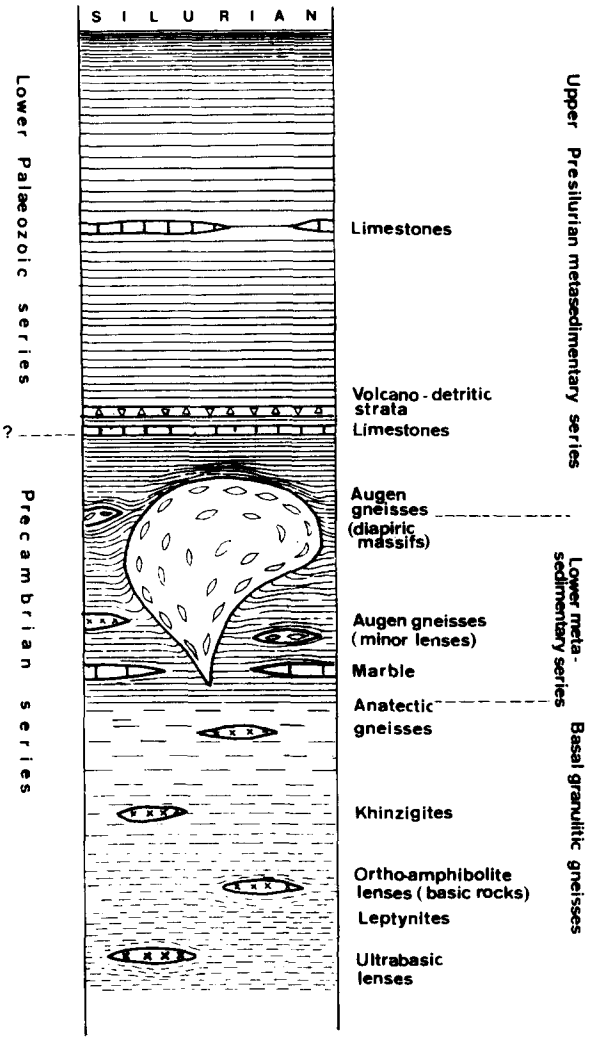


Fig. 2. Pre-Silurian rocks, synthetic 'stratigraphic' pile.

Déramond *et al.* 1971). An earlier foliation, defined by the preferred orientation of micas (mainly sericite) and chlorite plates parallel to the bedding and clearly apparent only in mica-rich rocks, was originally considered to be an *S*1 tectonic foliation. However, the majority of micas and chlorite plates can be shown to be detrital grains and, in the light of recent experiments on the deposition of mica plates, this foliation may have been due to depositional processes as well. Whatever it may be, this foliation which is apparent only in non-metamorphic or weakly metamorphosed terrains cannot be considered as the same as the major tectonic foliation which is seen in micaschists and gneisses from the higher metamorphic zones.

*Deformation* D2

The second deformation, *D*2, has formed the major regional folds, *F*2, and the major regional foliation, *S*2 (Figs. 3–5). The axial planes of *F*2 folds and the *S*2 foliation are steeply inclined and are N 120°E to N 90°E trending where they have not been affected by superimposed later deformations. The axes of *F*2 folds are, in general, gently inclined.

The shape of the *F*2 folds and the morphology of the *S*2 foliation change markedly as a function of metamorphic grade and this is of major interest for understanding the relationships between deformation and metamorphism and the origin of the domes.

As metamorphic grade increases, *F*2 folds become more amplified and more flattened in the same rock type. This evolution has been followed numerically by measuring sections perpendicular to the axis and determining the class of the folds (Ramsay 1967, p. 359). The shape has been studied by means of harmonic analysis of the profile according to Hudleston (1973). In order to allow statistical studies, the fold class has been determined on $t'^2_\alpha - \cos^2\alpha$ graphs (Hudleston 1973) instead of the $t'_\alpha - \alpha$ graphs of Ramsay. On these graphs, parallel folds modified by homogeneous flattening are represented by straight lines and can be described by the intercept of the best fit line of its representative points (Hudleston 1973). It has been found that the representative points of the *F*2 folds are often rather close to the best fit line. This is especially true for layers with low ductility contrasts and suggests that most of *F*2 folds are probably flattened parallel folds. Therefore, the closer the 'average' class of *F*2 folds to fold class 2, the greater the amount of homogeneous shortening superimposed on parallel folds, or, in other words, the closer the intercept to zero, the greater the amount of homogeneous shortening (see Fig. 6).

According to Hudleston (1973), the shape of the fold profile has been represented by the first (odd) sine Fourier coefficient, $b1$, which is close to the amplitude/wavelength ratio, and the ratio of the first and third odd Fourier coefficients, $b3/b1$, which is characteristic of the type of the fold (the ratio is zero for sine waves). An increase of $b1$ indicates an increase of amplification.

More than 3000 *F*2 folds have been measured on more than 50 stations. The results are expressed as frequency diagrams (Fig. 6). For clarity, only two main lithologic types and two metamorphic zones have been distinguished. Each diagram on Fig. 6 thus represents about 200–300 folds, which minimizes the influence of local variations.

The diagrams clearly show an increase of both homogeneous shortening and amplification of *F*2 folds, that is of finite strain, with increasing metamorphism. The same trend can be shown, if only qualitatively for *S*2 foliations.

In areas of low metamorphic grade, the *S*2 foliation is represented by crenulations with large spacing, open microfolds and rather weak differentiation. Tectno-metamorphic banding (= differentiation banding) is very poorly developed. With increasing metamorphic grade, the crenulations become more closely spaced, the microfolds more amplified and a well-contrasted tectono-metamorphic layering is common as the *S*2 foliation (Soula & Debat 1976). In areas of higher metamorphic grade (lower biotite–upper andalusite and higher) tectono-metamorphic layering becomes still more marked, giving rise to a 'false-bedding' which has often obliterated the original (sedimentary) bedding. In some cases, tectono-metamorphic layers consisting almost


Fig. 3. Structural map of the Pyrenees in the Ariege region. Dip symbols represent *S2* regional major foliation in sedimentary rocks and gneisses and the primary foliation (corresponding to *S2*) in plutonic rocks. Values shown on the map have been averaged after graphical restoration to the effects of the later deformation phases. Thin interrupted lines are traces of *S2*. *F2* folds having sub-horizontal plunge and trend parallel to *S2* are not represented by special symbols. For clarity, the majority of the Alpine faults have been omitted. Key: (1) Post-Hercynian rocks; (2) Pre-Hercynian sedimentary and metasedimentary rocks; (3) Migmatized micashists; (4) Augen gneisses (major massifs); (5) Augen gneisses (minor stocks including Prayols massif); (6) retromorphosed granulite facies gneisses ('granulitic' gneisses); (7) Basic and ultrabasic rocks; (8) Plutonic massifs and (9) anatectic granites.

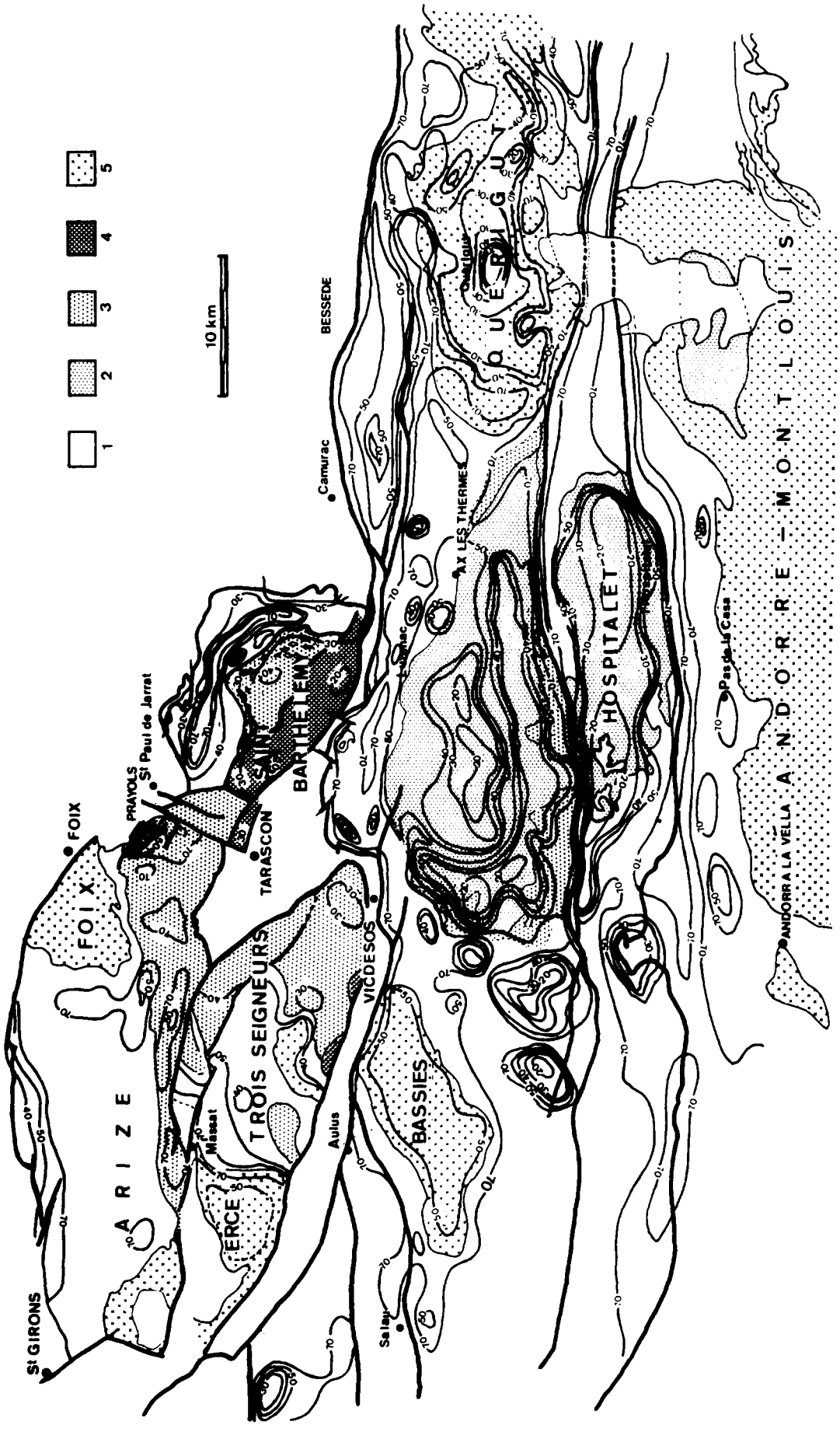


Fig. 4. Dip isogon contouring for $S2$, same area as Fig. 2. Top of the numbers directed towards steeper dip areas. Key: (1) Pre-Hercynian sedimentary and metasedimentary rocks; (2) Augen gneisses; (3) Migmatized micashists; (4) Granulitic gneisses and (5) Plutonic massifs.

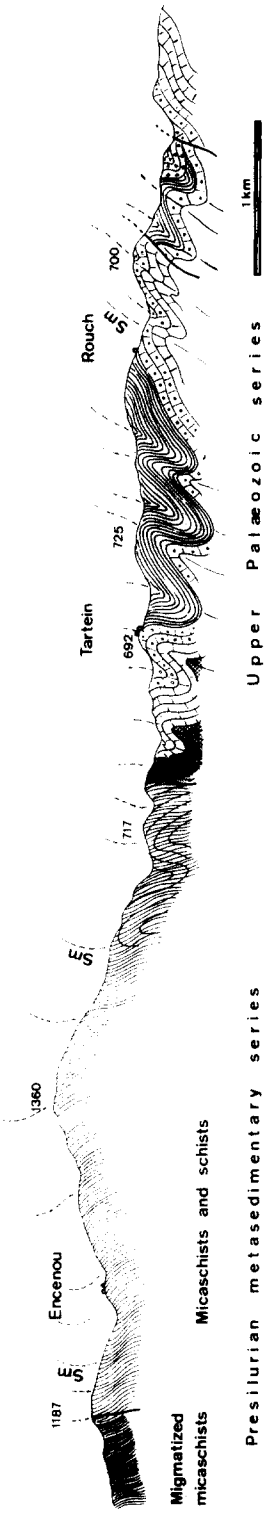


Fig. 5. Structural cross-section through central Arize, no gneiss massif is involved in the structure (modified from Barrouquère 1968, for Upper Palaeozoic terrains and from Castaing 1972, for pre-Silurian terrains). The section is situated to the west of the sections in Fig. 11. See caption for Fig. 8.

entirely of andalusite have formed in this manner. The crenulations progressively grade into well-developed schistosities which result from (i) the evolution of domainial crenulations where the mica-zones separating the microlithons become comparatively larger and more closely spaced, (ii) the mechanical reorientation of pre-existing micas, (iii) the tightening of microfolds to isoclines, most often with recrystallization in the hinges or (iv) the oriented growth of new minerals evenly distributed throughout the rock (e.g. biotite, andalusite, sillimanite), directly oriented parallel to the foliation and axial planes of folds, and cross-cutting older deformed minerals.

*Deformation* D3

The third deformation, *D*3, is responsible for upright folds, *F*3, with amplitudes and wavelengths ranging from microscopic dimensions to hundred of metres and locally to more than 1 km (e.g. south-western boundary of the Aston massif, Fig. 3). *S*3 foliation is represented by crenulations with locally tight microfolds or close spacing of mica films separating the microlithons. Differentiation may be locally well-marked but no *S*3 tectono-metamorphic false-bedding can be seen. In some cases, reorientation of mica plates or oriented growth of new biotites can give rise to strong preferred orientations which obliterate the older structures and a careful examination is needed to distinguished this foliation from *S*2 foliation.

On a regional scale, the axial planes of *F*3 folds and *S*3 foliation show statistically a sigmoidal attitude, swinging from N 90–120°E to N 150–160°E, depending on their distance from the major faults which run parallel to the direction of the Pyrenean chain (the Merens fault or the North-Pyrenean fault). Close to the faults, *F*3 folds become tight and pass into sheath folds in the fault zone. *S*3 foliation also grades into mylonitic foliation within the fault zone. This has led them to be considered as related to sinistral strike–slip shearing, the continuation of which later gave rise to the faults (Aparicio *et al.* 1975, Lamouroux *et al.* 1981).

*Deformation* D4

The fourth deformation, *D*4, is responsible for folds, *F*4, ranging from open undulations and kink-bands, to tight chevron folds, with gently inclined axial plane. The folds occur on all scales and locally are responsible for the flat-lying attitude of older structures on a kilometric scale. *S*4 foliation is a crenulation, in general with large spacing (about 1 cm or more) but locally with close spacing (less than 1 mm).

*Later deformations*

In addition to the major Hercynian deformations, later structures can be seen in pre-Hercynian terrains. Some of them are obviously Alpine structures (Soula & Bessière 1980, Lamouroux *et al.* 1980, 1981). The most

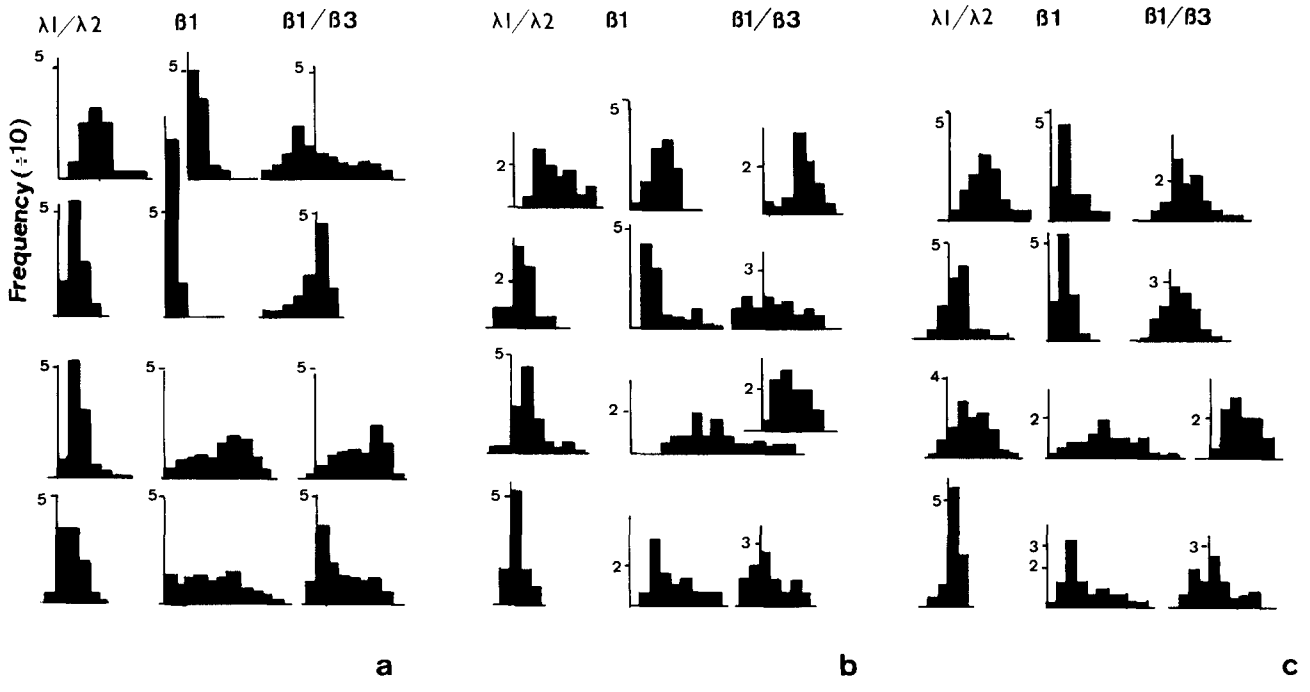


Fig. 6. Statistical representation of $F2$ folds in three characteristic areas. (a) Arize massif, central part of the massif outside the contact of gneissic and plutonic massifs. (b) Northern border of Aston massif. (c) Southern border of Hospitalet massif. Column 1 (on the left): Ramsay's (1967) fold class analysis, with the modified representation of Hudleston (1973). The folds are represented by the intercept of their representative lines on the $t'^2\alpha$-$\cos^2\alpha$ graphs as recommended by Hudleston (1973). Frequencies on the ordinate. Columns 2 and 3 (to the right): Harmonic representation using Hudleston's (1973) method. Column 2 shows the first Fourier coefficient, b1, in Fourier series development of the shape of the folds, and column 3 the ratio of the third and first coefficients, b3/b1. Line 1 (to the top): high-contrast rocks, chlorite and biotite zones; Line 2: low-contrast rocks, chlorite and upper biotite zones; Line 3: high-contrast rocks, andalusite and sillimanite zones; Line 4 (bottom): low- contrast rocks, andalusite and sillimanite zones. Note that flattening and amplification are stronger for the same lithological contrast between alternating layers at equal metamorphic grade for the folds to the North of Aston massif (b) and to the South of Hospitalet massif (c) than for the central Arize (a).

important are NW–SE trending mylonite zones corresponding to the sheared limbs of large-scale folds. The spacing of these mylonite zones ranges from a 100 m to 1 km (Lamouroux *et al.* 1981). For clarity the majority of these Alpine mylonite zones have been omitted in Figs. 3 and 4. Other structures are much more difficult to date and, on account of their poorly-defined characteristics and of their scarcity, an attempt to group them into deformation phases is illusory.

*Relationships between regional metamorphism and deformation*

Regional metamorphism occurred throughout the whole structural history. It can be shown that the peak of progressive metamorphism was attained during the major deformation $D2$ in all structural levels (Soula 1971, Déramond *et al.* 1969). This interpretation is in agreement neither with that of Guitard (1970) nor that of Zwart (1968, 1979). The principal arguments which support it are the following:

(1) The development of $S2$ foliation may be due to the oriented growth, parallel to $S2$, of new biotite crystals evenly distributed throughout the rocks and cross-cutting older mica crystals which have been folded by $F2$ microfolds.

(2) Oriented growth of elongated andalusite or sillimanite crystals parallel to $S2$ which are boudinaged by $S2$. In some cases andalusite crystals are seen as very elongated crystals, with dimensions in sections parallel to the $c$ axis of about 100 × 2–3 mm and, occasionally 50 × 1 cm. These crystals form true andalusite layers, where the andalusite content is greater than 70–80%, alternating with quartzitic layers. The crystals are very rich in inclusions and have diffuse boundaries with the matrix. The study of the progressive development of the andalusite layers with increasing metamorphic grade strongly suggests than they developed as tectono-metamorphic layers, i.e. by metamorphic banding induced by tectonic differentiation, in the same manner as other $S2$ metamorphic layering (Soula & Debat 1976).

(3) Sillimanite developed on previous andalusite crystals boudinaged by $S2$, occurs firstly on the edges of the andalusite crystals, i.e. in higher pressure zones.

(4) Andalusite and staurolite porphyroblasts often contain $S2$ foliation as inclusions while they are contoured and boudinaged by the same $S2$ with pressure shadows well-developed. Included $S2$ ($S2$i) is often less well developed than external $S2$ ($S2$e), or $S2$i is still a crenulation whereas $S2$e is a schistosity with preferred orientation of micas.

(5) Early-stage migmatitic veins, which can be shown to have formed in response to the same mechanism as tectono-metamorphic banding (Robin 1979) are seen

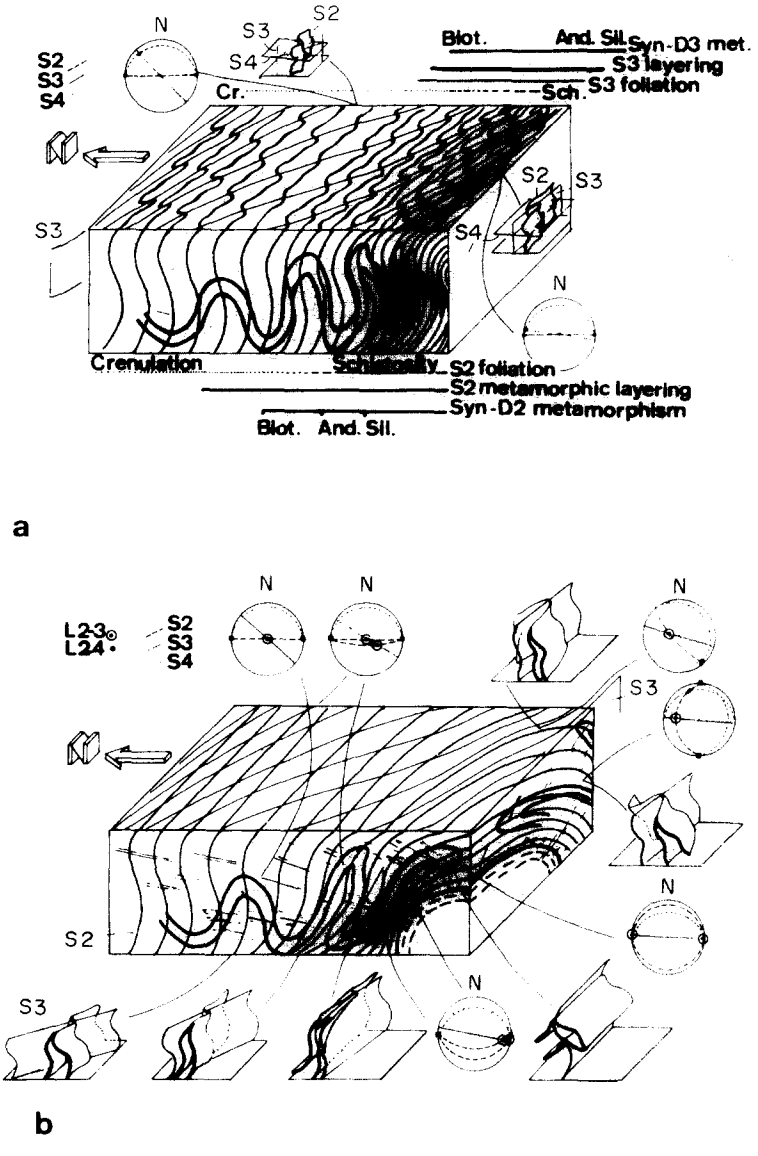


Fig. 7. Schematic evolution of $D2$ structures and attitude of post-$D2$ structures related to the attitude of $S2$. (a) Outside the contacts of the domes; (b) nearing the domes. In (a) the evolution of the $S2$ foliation, the appearance of a $S2$ metamorphic layering, and the syn-$D2$ metamorphic isograds are shown.

parallel to $S2$.

(6) The earliest anatectic granitoids are affected by $S2$ (Soula 1969).

The evolution of $F2$ folds and $S2$ foliation with increasing metamorphic grade, as reported above, is also a strong argument in favour of the proposed interpretation.

However, regional metamorphism can be shown to have still been active after the $D2$ deformation and during the $D3$ deformation:

(1) The last biotite plates to crystallize are oriented parallel to $S3$ in the deepest structural levels.

(2) Some andalusite crystals occur parallel to the axial planes of $F3$ folds, including hinges of some $F3$ microfolds. It should be stressed, however, that in most of the cases, the orientation of andalusite crystals parallel to the axial plane of $F3$ folds is due to a mechanical reorientation of andalusite crystals initially parallel to $S2$.

(3) Several generations of later anatectic veins can be shown to have developed during the progressive development of $F3$ folds.

However, the metamorphism appears to have been less widespread during $D3$ than during $D2$ and is restricted to areas closer to the core of metamorphic domes. At a given structural level, it can be shown than syn-$D3$ (or late $D3$) metamorphism was a retrogressive metamorphism, in contrast to the assertion of Zwart (1968, 1979). Moreover, in terms of the magmatic evolution of anatectic melts, the late-$D3$ anatectic veins are only late products (e.g. albite–microcline or albite–muscovite pegmatoids).

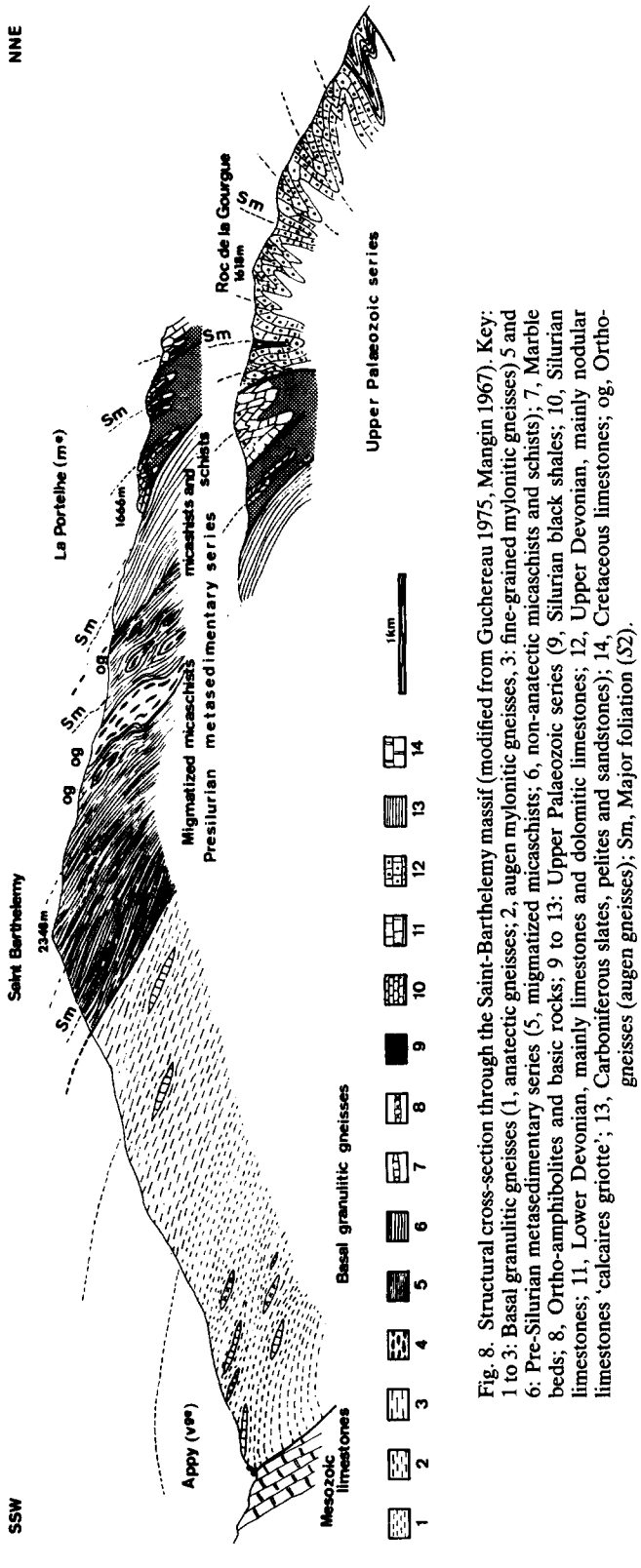


Fig. 8. Structural cross-section through the Saint-Barthelemy massif (modified from Guchereau 1975, Mangin 1967). Key: 1 to 3: Basal granulitic gneisses (1, anatectic gneisses; 2, augen mylonitic gneisses; 3: fine-grained mylonitic gneisses) 5 and 6: Pre-Silurian metasedimentary series (5, migmatized micaschists; 6, non-anatectic micaschists and schists); 7, Marble beds; 8, Ortho-amphibolites and basic rocks; 9 to 13: Upper Palaeozoic series (9, Silurian black shales; 10, Silurian limestones; 11, Lower Devonian, mainly limestones and dolomitic limestones; 12, Upper Devonian, mainly nodular limestones 'calcaires griotte'; 13, Carboniferous slates, pelites and sandstones); 14, Cretaceous limestones; og, Orthogneisses (augen gneisses); Sm, Major foliation (S2).

## COMPOSITION, SHAPE AND STRUCTURE OF THE DOMES

### *Granulitic gneiss domes*

Granulitic gneisses are aluminous paragneisses with some boudinaged and deformed charnockites or basic rocks. At the base of the Castillon massif, intrusive but deformed ultrabasic rocks are also exposed.

Granulitic gneisses form the cores of structural-metamorphic domes which, on the map, have an elongate shape (Figs. 3 and 4). Only part of each gneiss dome is seen, but, from the exposed structures, their dimensions may be estimated to be about 30 × 20 km. In vertical cross-sections, the part of the domes accessible to observation shows a typical arcuate shape (Fig. 8). The relationships between the cover rocks and the granulitic gneiss core may be best observed in the Saint Barthelemy massif. On the map, the major lithologic boundaries, the major foliation and the axial planes of the major folds in the cover rocks are grossly parallel to the contours of the basement–envelope interface and to the foliation in the basement gneisses. In vertical cross-sections, the lithologic boundaries, the foliation and the axial planes of folds all show a characteristic fan shape, the dips being very shallow near the centre of the dome and becoming increasingly steeper (and occasionally overturned) towards the external zone.

Mylonite zones delineate the major lithologic boundaries, both in the envelope and in the gneisses. The most important of them occurs at the contact between the gneisses and the envelope, and is common to the gneisses and envelope alike. In the gneisses, it has a thickness of some hundred of metres (Guchereau 1975, Passchier 1980). In fact, it can be shown that mylonitization gradually develops in the gneisses over a much greater thickness (more than 1–2 km in the Saint Barthelemy massif). The mylonitization can, in this respect, be considered as the ultimate result of progressive deformation with maximum strain set up at the outer boundary of the gneiss dome. Moreover, the gneissic foliation appears to be a composite foliation formed by the superposition of several minor deformation phases, probably as the result of a single progressive deformation (Soula & Guchereau, unpublished). The relationships between the successive structures forming this foliation appear rather similar to those expected from Dixon's (1975) experiments or Cobbold & Quinquis' (1980) theoretical and experimental predictions. Gneissic banding is likely to have been the result of the first stage of progressive deformation, and is suspected to be also a mylonitic structure. It should be stressed that the mylonites which are referred to in this section are early mylonites, clearly related to the dome structure, which must not be confused with the much later NW–SE trending mylonite zones described in the preceding section which cross-cut the dome structure and which have been found to be Alpine in age.

From the petrological viewpoint, granulite gneisses

are characterized by the co-existence of granulite facies and amphibolite facies assemblages. They have been considered by some authors to be the result of progressive metamorphism (e.g. Autran *et al.* 1966, Fonteilles 1976, Guitard 1977). However, as pointed out by Roux (1968, 1977), Guchereau (1975) and El Hourani (1980), the mutual relationships between minerals and between minerals and structures show that a retrogressive amphibolite facies metamorphism has been superimposed on an older granulite facies metamorphism in all types of rocks. Recent observations (El Hourani 1980 and personal observations) lead to the conclusion that the foliation developed progressively during the retrogression of high pressure assemblages into lower pressure assemblages. In the Saint Barthelemy massif, it can be shown that deformation continued under lower temperature conditions, inducing the most apparent mylonite zones.

The decrease in pressure has been estimated by Roux (1977) from petrological considerations as from more than 10 to 7 kb in the Castillon massif, which corresponds to the deepest part of the exposed granulitic gneisses. In the Saint Barthelemy massif, from estimates of the thickness of the terrains overlying the granulitic gneisses, the depth is likely to have been not more than 10 km, so that maximum pressure cannot have been more than 3–4 kb at the time of the emplacement of the gneiss dome in the metasedimentary series. This value is in agreement with the observed mineral reactions at the base of the metasedimentary series and at the top of the granulitic gneisses (Zwart 1953, Soula 1969, Guchereau 1975). This suggests that the granulitic gneisses have been uplifted about 20 km, which is close to the quarter-wavelength (in fact, the half-span) of the massifs.

*Augen gneiss domes*

The augen gneisses are rather homogeneous acidic granitoid gneisses exhibiting a typical augen structure developed around variably deformed and recrystallized K-feldspar megacrysts. These gneisses have been shown to have been derived from the deformation of pre-Hercynian granitoids (Martignole 1964, Jaeger & Zwart 1968, Guitard 1970, Debat *et al.* 1975, 1978). Recent microstructural studies supported by TEM investigations have shown that, in gneisses of this type, the augen structure and the foliation developed at the same time as the high temperature dynamic recrystallization of K-feldspar megacrysts (Vidal *et al.* 1980), i.e. during high temperature metamorphism.

The augen gneisses form domes with dimensions ranging from 1 km to several kilometres, but they occur also as smaller massifs, lenses or sills with dimensions ranging from 1 to 100 m, with the same composition and structure. It should be noted (and this is of interest in the interpretation of the domes) that the small massifs, the lenses and the sills are restricted to the basal part of the pre-Silurian metasedimentary series whereas large sized domes, where present, are situated at higher structural levels.

The domes show intrusive structural relationships with the enclosing rocks and the contacts are, in general, mylonitized. It can be shown that the gneissic foliation gradually passes into the mylonitic foliation toward the margins of the domes with increasing flattening of grains and/or increasing recrystallization. The foliation in the gneisses and the major regional foliation in the envelope are nearly parallel. Because of the mylonitized contacts, it cannot be established with certainty from continuity arguments whether the gneissic foliation is the analogue of the major regional foliation, or an older foliation affected by a younger coaxial deformation. Indirect arguments, however, strongly suggest that the gneissic foliation corresponds to the major foliation in the envelope: (1) the major foliation in the country rocks is seen to be in continuity with the gneissic foliation of the minor lenses or sills of augen gneisses interlayered with metasediments and (2) TEM studies of Vidal *et al.* (1980) have shown that the gneissic foliation developed during the peak of metamorphism as did the major foliation in the country rocks.

Two examples of gneiss domes, the Aston massif and the Prayols massif are shown in Figs. 9–13. Three-dimensional reconstructions show that both have a characteristic mushroom shape and are elongate parallel to the regional trend of the regional major foliation. The Aston massif is markedly asymmetrical both in N–S and E–W cross-sections (Fig. 9).

In these gneisses, anatexis and recrystallization, together with the heterogeneity of later deformations do not permit a systematic study of finite strain ellipsoids. However, the shape of the augen, orientation of preserved megacrysts (in the zones where their concentration is low, see Debat *et al.* 1975) and the shape of quartz nodules allow, some approximate estimates of the type of the ellipsoid. It has been found to be of oblate (flattening) type ($0 < K < 1$). The lineation is rather weak and often obliterated by recrystallization and anatexis. When observable it follows the contours of the domes.

*Plutonic domes*

The major plutonic massifs have usually an average composition of granodiorite, quartz–diorite or monzogranite but some of them show a wider range of rock types, from leucogranites to gabbro-norites and occasionally cortlandites (e.g. Leterrier 1972, Marre 1973, Debon 1975). The origin of these plutonic rocks is still under discussion, some authors believing that they originated from differentiated and contaminated basaltic magmas (e.g. Autran *et al.* 1970, Marre 1973) while others consider that they originated from the generalized melting of a large part of the crust (e.g. Zwart 1968, 1979, Vitrac-Michard *et al.* 1980).

The massifs appear as a series of stocks, some kilometres in dimensions, intruded into Upper Palaeozoic and later pre-Silurian rocks. The three-dimensional shape is now rather well known (e.g. Marre 1973, Autran *et al.* 1970, Clin 1964, Barrouquère *et al.* 1976,

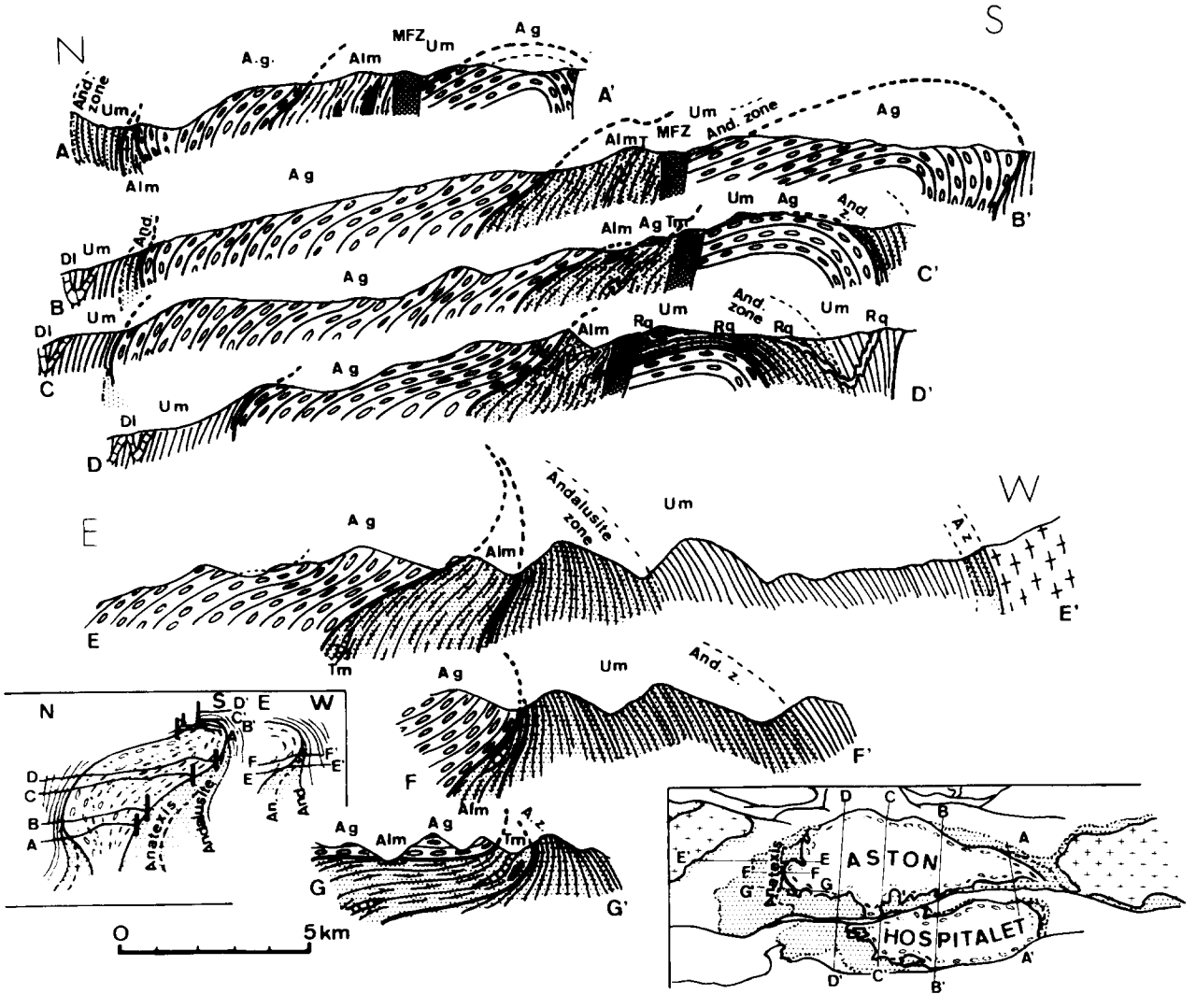


Fig. 9. Structural cross-section through the Aston–Hospitalet massif (after Soula 1979) Ag, Augen orthogneisses (Aston and Hospitalet gneisses); D1, Devonian limestones, Um, Upper pre-Silurian metasediments; A1 m, Anatectic lower pre-Silurian metasediments; Rq, Ransol quartzite (possibly Cambrian); Tm, Thoumasset marble; MFZ, Merens Fault Zone; crosses, Granitoid massifs; black, Basic and ultrabasic lenses and stippled, andalusite and sillimanite — K feldspar zones. Lower right, location of the sections on the map and lower left, location of the sections as function of their 'altitude' relative to the reconstructed overall structure. The upward and the left-lateral displacements of the lower northern part of the structure (exposed as Hospitalet massif) has been taken into account. On the sections, the NW–SE trending Alpine mylonite zones have been omitted for clarity.

Soula 1970, Lamoroux 1976). In some instances, the architecture of the massifs has been reconstructed from the disposition of internal structures. The best example is the Querigut massif (Figs. 14, 15 and 16) where detailed structural analyses have been carried out (Marre 1973, Laffont 1971, Pons 1971). From these studies it can be shown that the external boundaries and the foliation, both in the granitoids and the envelope, define conformable mushroom shapes on a regional scale. Cross-cutting relationships are occasionally seen on the scale of an outcrop between the different rock units constituting the massif, but they are only local and of minor importance. The main rock-types have a well defined position relative to the overall structure of the massif; granitic rocks, constituting the major part of the intrusive are situated in the core; granodioritic rocks are at the periphery, making up the southern and western margins; gabbro-dioritic rocks and the less frequent mafic rocks appear as rounded to lenticular xenoliths within the other rock-types. Deformed and metamorphosed sedimentary xenoliths are also seen towards the margins. The material on the periphery is intensely sheared and the primary foliation ('magmatic'? foliation) progressively passes into mylonitic foliation towards the outer boundaries. Lineations and other linear structures, as determined by Marre (1973), are, in general, perpendicular to the contours of the massif (Fig. 16). The foliations are believed by Marre (1973) to be characteristic of liquid magma flow. Structural observations and more general considerations (see below), led us to consider them as having been formed by the deformation of magma in a highly crystallized state (Soula & Borrel 1980, see also Berger & Pitcher 1970).

Several other Pyrenean plutonic massifs have been

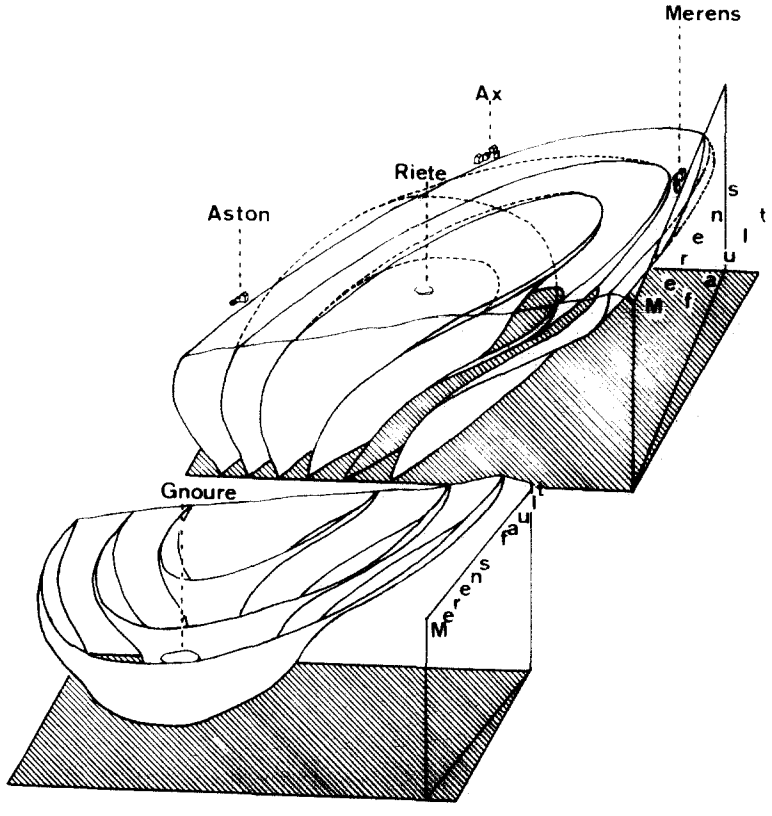


Fig. 10. Spatial reconstruction of the Aston–Hospitalet massif.

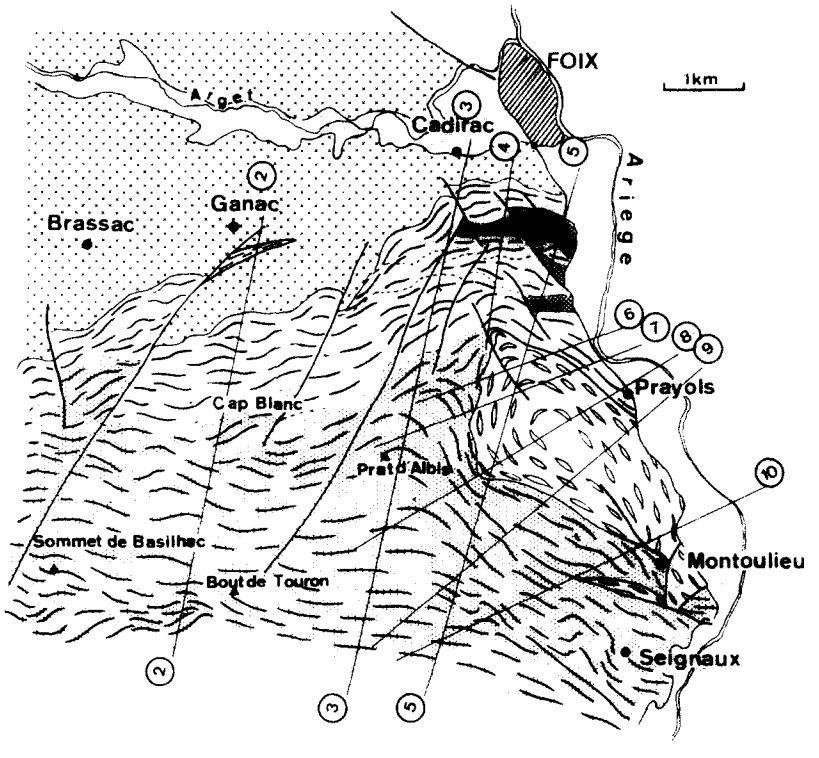


Fig. 11. Detailed map of the eastern Arize massif (modified from Soula 1969). Dark-stippled areas, Silurian slates; white, Pre-Silurian schists and micaschists (chlorite zone to muscovite–sillimanite zone); light-stippled areas, migmatized micashists (K feldspar–sillimanite zone); elongate nodules, Augen gneisses (Prayols massif); crosses, Granodiorite (Foix massif). The thick interrupted lines and the long axes of the nodules represent the trace of $S2$ foliation and the trend of $F2$ fold axes. For clarity, NW–SE trending Alpine faults and mylonite zones have been omitted. Numbers and lines refer to cross-sections in Fig. 12.

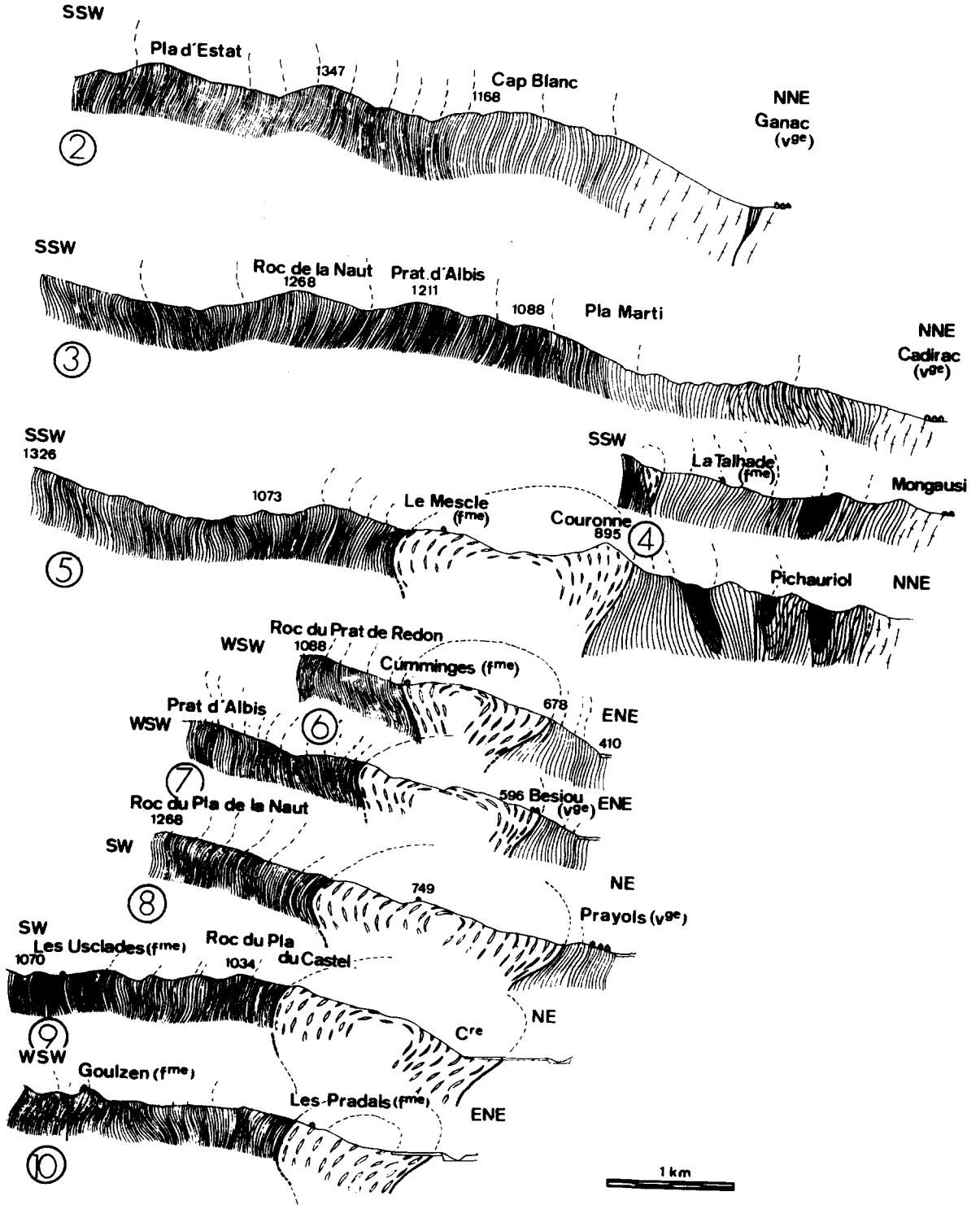


Fig. 12. Structural cross-sections through eastern Arize massif. The location of the sections is shown in Fig. 11. For key, see Fig. 11.

shown to have similar asymmetrical mushroom- or inverted pear-shaped forms, although they have not been studied in the same detail as those described here.

## RELATIONSHIPS BETWEEN THE DOMES AND THE REGIONAL STRUCTURES

### *Deformation around the domes*

Around the domes, one can see the same succession of deformations as in dome-free areas, but with significant differences in orientation and development.

The most significant differences are shown by the *D*2 and *D*3 phases.

In the case of the *D*2 phase, the axial planes of *F*2 folds and the *S*2 foliation become progressively parallel to the contours of the domes, as margins of the domes are approached, passing from a vertical to a horizontal attitude towards the top or the overturned margins of the domes, and from an E–W to a N–S trend at the contact

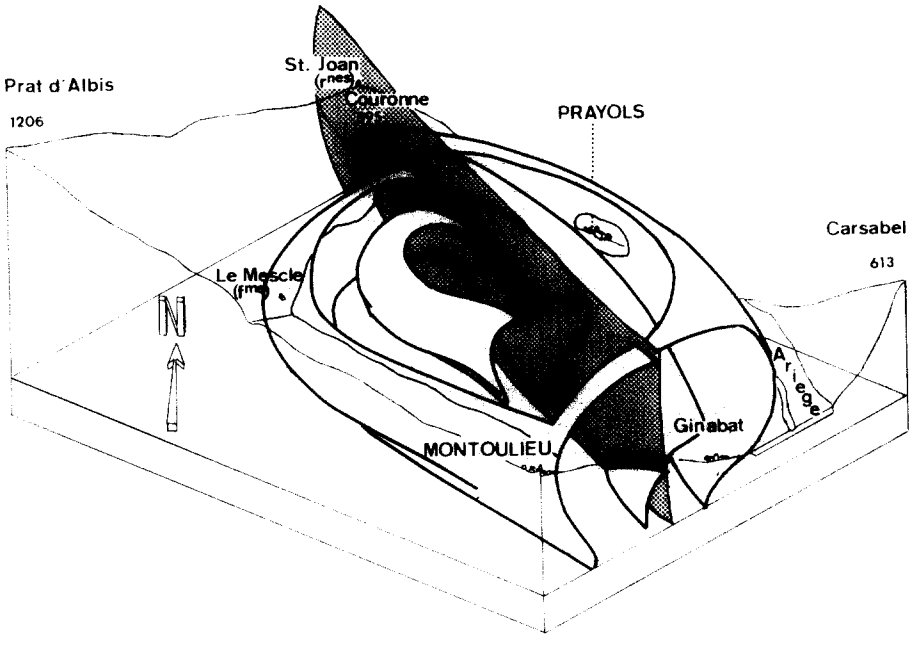


Fig. 13. Spatial reconstruction of Prayols augen-gneiss massif. Thin lines represent the actual topography; thick lines represent the boundaries of the massif and the structure within the massif as shown by the disposition of the foliation. The lines with intermediate thickness represent the intersections between the enveloping surface of the gneisses or their foliation and the actual topography. The locality names refer to the 1/25 000 topographic map of the France IGN editor, sheet: Foix).

of eastern and western edges of the domes (Figs. 3 and 4). The axes of $F2$ folds remain close to horizontal but their direction still becomes parallel to the contours of the domes, progressively passing to N–S on the eastern and western edges of the domes, i.e. taking a direction perpendicular to their regional trend. At the same time the amount of strain, as recorded by $F2$ folds, increases towards the domes, becoming markedly higher than in dome-free areas for the same metamorphic grade and the same rock-type (the arithmetric mean for flattening component and amplification of $F2$ folds is higher for each rock-group and each metamorphic zone, Fig. 6). Qualitatively, this increase in strain leads to the development of the mylonites seen at the contact with the domes. Some, parasitic folds are also exposed, the asymmetry of which indicates either normal uplift (e.g. northern Aston) or overthrusting (e.g. southern Aston, Querigut pluton), in agreement with the overall structural situation. The mylonitization in the gneisses and in the envelope seems to have been due to the same mechanism within and around the domes, and may be considered to have been the ultimate result of the $D2$ deformation.

In the case of $D3$ deformation, the axial planes of $F3$ folds and the directions of maximum shortening axes for $F3$ kink-bands, as estimated by Aparicio & Lelubre (1976), deviate relatively slightly but significantly around the domes. The most significant variation is, however, that of the inclination of $F3$ fold axes where: $S2$ is flat-lying, i.e. commonly in the central part of the domes or in their overturned margins, $F3$ fold axes are gently inclined; $S2$ dips steeply, i.e. — the margins of the domes are vertical, $F3$ fold axes are steeply inclined whatever the strike of $S2$; $S2$ has an intermediate dip and $F3$ fold axes have intermediate inclinations. These relationships are schematized in Fig. 7. They indicate that the domes were developed before $D3$.

*Relationships between deformation and contact metamorphism and time of emplacement of plutonic granitoid domes*

In the Pyrenees plutonic domes have been often considered to have been late-stage events with respect to the Hercynian deformation. As a demonstration of this, it has been argued either that granitoids are cross-cutting to the regional structures, developing a static contact metamorphism (e.g. Autran *et al.* 1970, Zwart 1968, 1979) or, on the contrary, that regional structures actually contour the massifs, this being interpreted as due to a pushing aside of regional structures by the pluton (Marre 1973).

A detailed study of the contacts of most of the granitoid plutons has shown that the granitoid massifs are contoured by the major $S2$ foliation on a regional scale, and are affected by the $D3$ deformation in the same manner as the gneiss domes (Aparicio *et al.* 1975, Lamouroux 1976, Soula 1979, Lamouroux *et al.* 1981). Apparent cross-cutting relationships are most often due to a fault contact or the local emplacement of late magmatic products. It should be stressed, however, that even when a granitoid cross-cuts a foliation which regionally contours it, this cannot be taken as an argument to demonstrate the late emplacement of the granitoid relative to the development of the regional structure. Indeed, experiments on diapirism (e.g. Ram-

berg 1967, 1970) and observations of salt domes clearly show that mature diapirs commonly cross-cut the structures which they induced during their uplift (see also Figs. 22–24). Moreover, it seems rather unlikely that granitoids could have been emplaced as a whole at one time. They are more likely to have had a complex and polyphase emplacement history, with, for example, successive emplacements of magmas of unlike composition or episodic magmatic pulses (see, e.g. discussions in Elder 1970 or Pitcher 1979). Structural studies of Pyrenean granitoids strongly suggest such a complex emplacement history (Autran *et al.* 1970, Marre 1973, Soula 1970).

In addition to the fact that the overall relationships to regional structures are the same for granitoid massifs and gneiss domes, it can be shown that contact metamorphism has the same relationships to regional deformation as regional metamorphism, with the peak of contact metamorphism contemporaneous with the major regional *D*2 deformation and with retrogressive metamorphism occurring during and after *D*3 (Soula 1970, Laffont 1971, Castaing *et al.* 1973, Aparicio 1975, Lamouroux 1976, Barrouquère *et al.* 1976). The evolution of *S*2 and *S*3 regional foliations towards the granitoid massifs is comparable with that seen as one approaches areas of increased regional metamorphism, and especially, the development of *S*2 tectono-metamorphic banding. Furthermore, in certain cases, the isograds of contact metamorphism pass continuously into the isograds of regional metamorphism (Soula 1970, Castaing *et al.* 1973, Barrouquère *et al.* 1976). All these observations show that the granitoid massifs were emplaced essentially during the *D*2 regional deformation, only late magmatic events are actually younger than *D*2 deformation. However, the contact metamorphic history is believed to reflect the complex emplacement history of the magmas (Soula 1970).

On account of its attitude, conformable to *S*2 at the margins of the plutonic domes, the primary foliation in the granitoids may be considered also as an analogue of the *S*2 foliation in the country rocks.

## DIAPIRIC ORIGIN OF DOMING

Gneiss domes have been attributed either to buckling (interfering cross folds with dome and basin patterns, e.g. Ramsay 1967, or non-cylindrical folding) or to diapirism.

In the Pyrenees, the buckling hypothesis has been supported by some authors, who invoke interfering (superposed or simultaneous?) late folds (e.g. Guitard 1970, 1977), or anticlinal (non-cylindrical?) folding (e.g. Seguret & Proust 1968 a, b). These interpretations assume that the major regional foliation was initially horizontal everywhere.

The hypothesis of diapirism now seems to be widely accepted for plutonic intrusions, and in the Pyrenees has been proposed by Marre (1973) for the Querigut intrusion.

The criteria used in most structural studies to distinguish between buckling or diapirism are based on finite strain measurements. These criteria are, however, sometimes equivocal (e.g. discussion in Schwerdtner *et al.* 1978). They are often difficult to apply in areas of progressive deformation (e.g. Dixon 1975), where strong later deformation has been superimposed on the dome structure, or when strain markers are lacking or have been obliterated by recrystallization or anatexis. Since such difficulties occur in the area studied, the following discussion is based on specific local arguments.

From the observations reported earlier, it follows that the doming of *S*2 occurred before the *D*3 phase. As no other deformation occurred between *D*2 and *D*3, it follows that the dome structures were formed during the development of the *S*2 foliation.

In other words, the *S*2 foliation originated with a domed attitude and was not horizontal everywhere. Its attitude would have changed with progressive doming.

The variation in dip and orientation of the *S*2 and *F*2 folds contouring the domes, especially the fact that the *F*2 folds axes become progressively nearer to perpendicular with their regional trend, precludes an origin of the domes by refolding of the major *D*2 structures, either by cross-folding or by non-cylindrical folding. In fact, in the area studied, no cross folds with orientations and characteristics capable of giving rise to the domes have been observed. Furthermore, the mushroom shape of the gneiss domes and the similarity in shape of both gneiss domes and plutonic domes, together with the similarity of the structural relationships between both kinds of domes and their surrounding rocks, make it difficult to account for the doming in terms of interfering upright folds or non-cylindrical upright folding.

These similarities in shape, internal structure and relationships with enclosing rocks and regional structures strongly suggest that a single mechanism of doming was responsible for producing all the dome structures. The overall shape of the massifs, the development of mylonitic structures and the parasitic folds all suggest an intrusive uplift. The shape of both types of massif is very similar to those of diapiric domes in classical centrifuge experiments (e.g. Ramberg 1967, 1970, Dixon 1975, Talbot 1974, 1977, Schwerdtner & Tröng 1978), to those of other gneiss or plutonic diapirs (e.g. Martignole & Schrijver 1970a, b, 1977, Talbot 1974, 1977, Schwerdtner *et al.* 1978) or to those of salt domes (e.g. Trusheim 1960, Talbot 1979).

It appears, therefore, that diapiric uplift is the most likely mechanism of doming for the Hercynian Pyrenees. In fact, it seems difficult to envisage another mechanism of doming that would be common to both gneiss domes and plutonic massifs. The general increase in strain towards the boundaries of the domes both within the domes and the enclosing rocks agrees well, if only qualitatively, with the numerical models of Berner *et al.* (1972) or Fletcher (1972) and especially with the quantitative experiments of Dixon (1975). The disposition of planar and linear structures within the

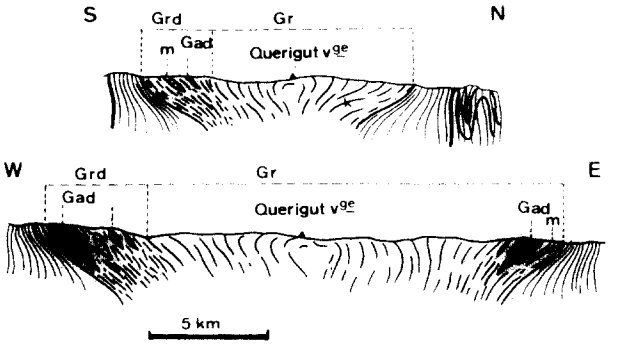


Fig. 14. Cross-sections through the Querigut plutonic massif. The sections have been constructed from Marre's (1973) data for the plutonic rocks and from Aparicio's (1975) data for enclosing rocks. Grd, Granodiorite; Gr, Granite; Gad, Gabbro-diorites; m, marble.

plutonic massifs, the estimates of strain and the orientation of lineations in augen gneiss domes are also consistent with this hypothesis. This would suggest either one or the other of the following:

(a) differences in erosion levels for gneiss and plutonic domes, i.e. in the diapiric structures, erosion has bitten down to levels nearer to the core for massifs such as the Querigut plutonic intrusion, and nearer to the crestal region for massifs such as Aston or Prayols (see discussion in Schwerdtner *et al.* 1978) and

(b) differences in the state of maturity of the diapirs and/or differences in the rate of strain linked to differences in rock properties. Further studies will be needed to elucidate this problem.

The marked decrease in pressure accompanying the development of the foliation and of the dome structure in granulitic gneiss massifs also strongly supports the hypothesis of diapiric uplift. As indicated earlier, the uplift of the granulitic gneisses was about 20 km, with a half-wavelength of the same value. This is compatible with the arched upper parts of the models of Dixon (1975). The progressive mylonitization at the top of these massifs is also in good agreement with these models.

The relationships between the regional deformation developed outside the domes, together with the elongate shape of the domes, parallel to the regional trend of *S*2 and *F*2 fold axes, suggest that the diapirism is likely to have occurred during major regional shortening. Some other recent studies suggest that diapirism during regional shortening should be rather common (e.g. Fyson & Fryth 1979, Ledru & Brun 1977, Brun 1980, Hanmer & Vigneresse 1980, Brun & Pons 1981).

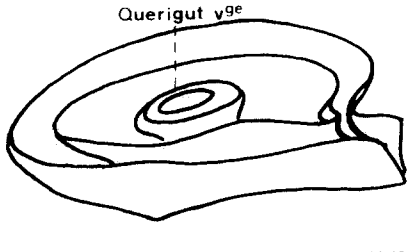


Fig. 15. Spatial reconstruction of the Querigut massif (from Marre's 1973 data).

## NATURE OF THE GRAVITATIONAL INSTABILITY

Fundamentally, diapirism implies gravity instability. The possibility of such a gravitational instability is, thus, often discussed in terms of gravity measurements and density measurements. However, these measurements are performed on the rocks in their present state and situation. In fact, it would be more important to have a knowledge of the gravitational instability at the time and place that diapirism was initiated. In the Pyrenees, gravity data are unfortunately not yet available on the appropriate scale. In the following discussion, it will be shown that gravity data, although convenient, are not essential to the interpretation.

Density measurements of metasedimentary rocks similar to those surrounding the domes have shown a mean value greater than that of granitoids even in the solid state. Values of 2.75–2.77 g cm$^{-3}$ have been quoted by Cooper & Bradshaw (1980), Wenk & Wenk (1969) and Ramberg (1980), whereas granitoids usually have densities of about 2.65–2.67 g cm$^{-3}$ and granodiorites densities of about 2.7 g cm$^{-3}$, in the solid state at room temperature and pressure. Again, it is well known that granites and granodiorites are often responsible for negative gravity anomalies. This is the case, for example, in the Aquitaine basin, to the North of the Pyrenees, where the pre-Hercynian terrains are the same as the Pyrenees and where geophysical surveying for petroleum exploration has been intense.

However, of greater interest in a discussion of the gravitational instability at the onset of the diapirism is a knowledge of the density differences in the conditions under which the diapirism may have developed.

Densities at room temperature and pressure of solid metasedimentary and eruptive rocks have been calculated from mineralogical compositions and densities of minerals. Data on mineral densities are from Robie *et al.* (1966). This procedure has been used in order to have homogeneous data for solid rocks and for magmas (see below). In doing so, the values are, in fact, very close to those usually given for mica-rich rocks (see e.g. Daly *et al.* 1966). Figure 17 gives average densities of the different rock units calculated by taking into account the relative abundance of the different rock-types in each of the different major rock-units. Densities at higher temperature and pressure have been obtained by calculating the thermal expansion and the compressibility of the rock-forming minerals (data Skinner 1966 and Birch 1966) and averaging for the observed rock compositions. It should be noticed that the coefficients of thermal expansion and compressibility are rather close for the major constituent minerals except quartz, the thermal expansion of which is about twice that of the other minerals. The density of quartz-rich rocks is, thus, expected to decrease much more than that of quartz-poor rocks with increasing temperature. In the calculations, thermal expansion and compressibility have been considered as independent variables. From the data compiled by Birch (1966), it appears that the compressibility

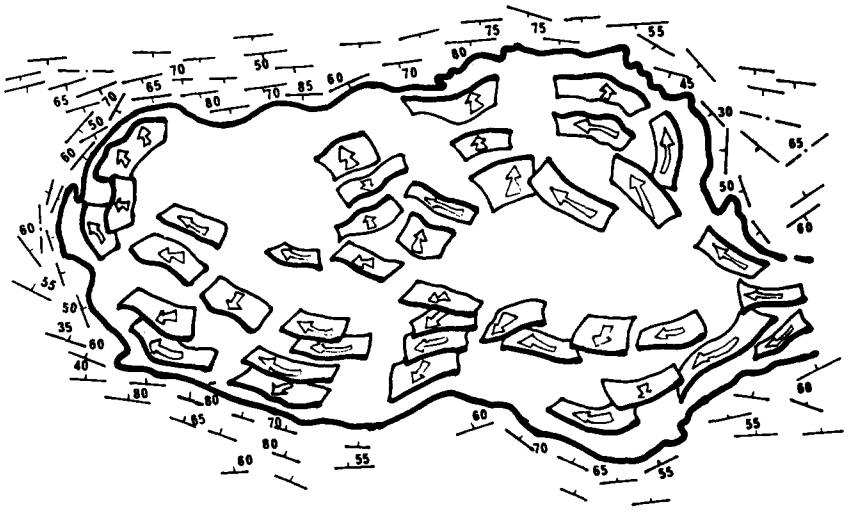

Fig. 16. Schematic of the kinematics of emplacement of the Querigut massif (after Marre 1973). The orientation of the *S*2 major regional foliation in the surrounding rocks are from Aparicio (1975). *F*2 fold axes, being parallel to *S*2 and sub-horizontal, are not represented.

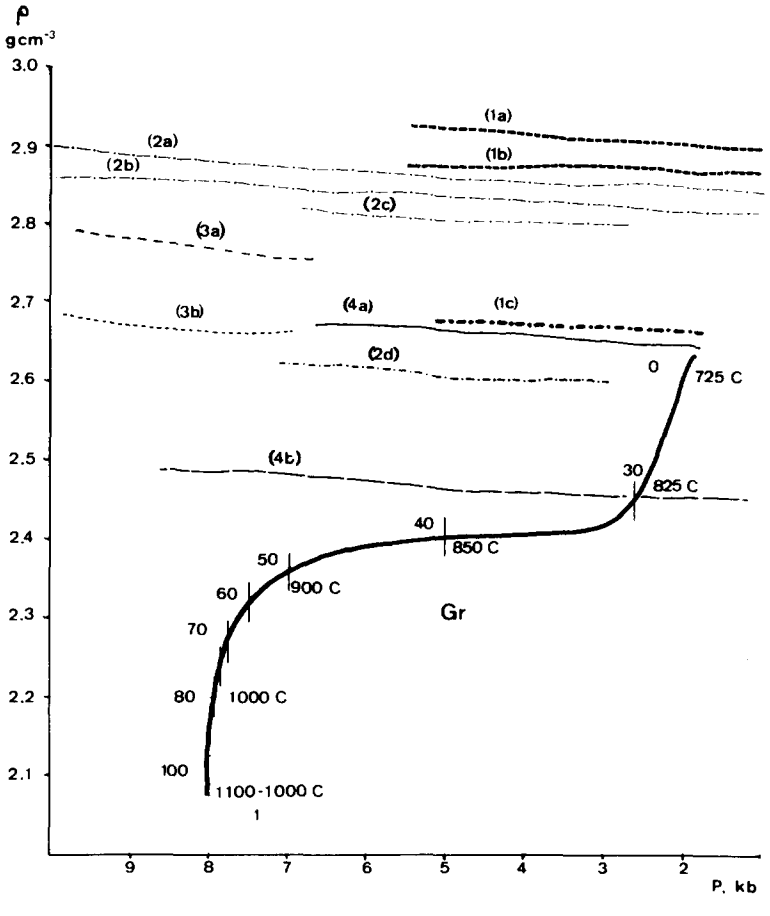


Fig. 17. Density of granitoids and country rocks as function of pressure and temperature. Gr., Granitic magmas, variation of density during the course of the crystallization, averaged for initial water content of the magma ranging from 0.6 to 3%. Numbers above the curve are melt fractions (in per cent). Numbers beneath the curve are corresponding temperatures (in °C). (1) to (4): Country rocks, values averaged for the different rock units by taking into account the relative abundance of each rock-type in each unit. (1a) Pre-Silurian metasediments, 400°C; (1b) the same, 600°C; (1c) the same, 700°C with 30% melt; (2a) Granulitic gneisses, secondary garnet-sillimanite assemblage, 400°C; (2b) the same, 600°C; (2c) the same, 800°C, 0% melt; (2d) the same, 800°C, 30% melt; (3a) Granulitic gneisses, initial hypersthene-kyanite assemblage, 700°C, 0% melt; (3b) the same, 700°C, 15% melt; (4a) Granitic augen gneisses, 600°C, 0% melt; (4b) the same, 30% melt. The curve for granitoid magmas has been computed by using Carron *et al.'s* (1978) program, applied to the studied granitoids on the basis of Borrel's (1978) petrographic observations. The composition of the initial and secondary assemblages of the granulitic gneisses are those determined by Roux (1977). The amount of melt has been determined from field and sample studies averaged for each rock unit.

of rocks, minerals or glasses varies only slightly with increasing P and T and it can be shown that the value of the density is not significantly altered by these variations. To the author's knowledge, no data are yet available on the variation of thermal expansion with pressure for rocks and they are assumed to be also rather small. In fact, such possible variation should be of little importance in terms of density differences, since densities at high P and T are computed in a similar way for all the types of rocks (including granitic magmas).

For granitoid magmas, density has been obtained by using the more sophisticated program elaborated by Carron and Dujon (Carron *et al.* 1978 and unpublished), which has been applied to the studied granitoids (Borrel & Soula, in preparation). The characteristics and the path of crystallization of the magmas as used in the calculation, have been established from petrographic and structural observations and the chemistry of major elements. P–T conditions were then deduced from Whitney's (1975) experimental data, corrected in order to take into account the crystallization of biotite (Borrel 1978). The granitoids studied were initially undersaturated in water (Borrel 1978). Since the actual initial water content cannot be determined with accuracy, the calculations have been performed for three possible values of initial water content. The results of the calculations are given in Fig. 17.

Density differences between granitoid magmas and the mica-rich upper metasedimentary series are rather large, even when considering that the magma was largely crystallized (density differences of about 0.5–0.3 g $cm^{-3}$) (Fig. 17). Furthermore, even the density contrast between liquid magmas and solid granitoids appears to have been sufficient to induce diapiric ascent.

It is very likely that, at pressures greater than 5–7 kb, country rocks were granulitic gneisses. Time relationships between the rise of the magmas now emplaced as granitoid stocks and metamorphism and anatexis cannot be determined for deep-seated areas and it is difficult to ascertain whether granulitic gneisses were partially melted. However, calculations taking into account the abundance of granitic veins in granulitic gneisses and considering that the veins were liquid, have shown that partial melting cannot have decreased the density by more than 0.1–0.15 g $cm^{-3}$. Therefore, the density differences are largely sufficient to induce a rapid diapiric ascent of the magma, no matter whether granulitic gneisses were partially melted (see Ramberg 1967, 1972, 1979 or Berner *et al.* 1972 for the control of gravity contrast on the rate of diapiric ascent).

The density contrast between the augen-gneisses and the enclosing metasediments is not so high (density differences of 0.2–0.3 g $cm^{-3}$ 600°C and 5–2 kb, Fig. 17) but it seems sufficient to have induced a significant rate of uplift. In addition, partial melting, occurring much more in the gneisses than in the surrounding micaschists, may have decreased the density (and also the strength, see van der Molen & Paterson 1979) of the granites, now appearing as augen-gneisses, much more than that of the micaschists. If, as pointed out by Roux (1977), partial melting was a result of uplift, the process of diapiric rise may have been 'self-accelerating', since partial melting should increase the rate of uplift and the uplift the amount of partial melting. The process is, of course, likely to have acted only while temperature remained sufficiently high, i.e. between 650 and 800°C (see above).

Instability could also be helped by thermal gradients (e.g. the thermal conductive models of Talbot 1974).

For the granulitic gneisses, the cause of the instability seems more evident. Three speculative hypotheses may be proposed.

(i) Diapirism developed as a result of the density contrast between hot deep-seated granulites and denser cooler overlying rocks (unexposed Precambrian cover and the exposed pre-Silurian series). From Fig. 17, the density difference could have been about 0.2 g $cm^{-3}$. In addition, if the basic sills and dykes in the Castillon massif resulted from basaltic magmatism older than the development of the foliation, as suggested by Roux (1977), this magmatism could have emplaced larger intrusions above the granulitic gneisses, thus increasing the gravitational instability. The diapirism would be helped by thermal gradients generated by deep-seated thermal domes. In this hypothesis, the ultrabasic rocks, which are also observed at the base of the Castillon massif (Roux 1977), could be initially deep-seated material (ultrabasic cumulates?) attracted by the rising diapir (e.g. Ramberg 1967, 1970).

(ii) The uplift of the granulitic gneisses would be a quasi-passive uplift driven by the diapirism of the upper mantle material. This could be due, for example, to the partial melting of the upper mantle, creating a gravititional instability by the lower density of the melted material (and helped by the viscosity contrast, see below). The ultrabasic rocks at the base of the Castillon massif could be evidence of this process. It should be noticed that from petrological and structural arguments Roux (1977) has considered the ultrabasic rocks to be responsible for an increase in temperature while the pressure was decreasing. The basic rocks may be products of an older magmatism and processes (i) and (ii) could have acted in combination.

(iii) The instability could have been created by partial melting of the crust, as suggested by Zwart (1968) and Vitrac-Micharg *et al.* (1980), and generated by heat rising from below, maybe as result of episodic thermal domes (e.g. Elder's 1970 models). Basic and ultrabasic rocks may be emplaced at various stages of the process, intruded from below, together with the thermal domes — which would be contrary to Vitrac-Michard *et al.'s* (1980) model — or attracted by the rising diapir. Ultrabasic bodies surrounded by higher grade contact metamorphism and local stronger anatexis in some metamorphic domes, favour an active role for the ultrabasic rocks. Opposing hypothesis (iii), it seems that no traces of granitoid magmas generated by crustal melting are discernible at the base of granulitic gneiss domes. However, as suggested by models (Fig. 24b), the granitoid magmas could have passed completely

through the granulitic gneisses via an open fracture system to be intruded at higher levels.

## ORIGIN OF METAMORPHIC DOMES

The problem of the origin of metamorphic domes seems directly linked to the discussion above. From the same arguments put forward here for the origin of gneiss domes, metamorphic domes cannot be interpreted as the result of interfering cross-folds or non-cylindrical regional folds, deforming flat-lying isograds, so that the dome shape of the metamorphic domes is believed to be original. Static models, such as 'basement effect' (Fonteilles & Guitard 1974), heat supply by radioactive reactions, static thermal exchanges with deep-seated materials, have been discussed and rejected, from general arguments, by Den Tex (1975) with special reference to the Agout dome in the nearby Montagne Noire. Instead, Den Tex suggests a large-scale crustal diapirism, based on Talbot's (1974) model of crustal convection in the solid state. A large-scale crustal diapirism, following Ramberg-type models, is also envisaged by Vitrac-Michard *et al.* (1980), apparently to explain the high metamorphic gradient and high decompression rates computed by Albarède (1976) from barothermometric data on Hercynian granulites in the Massif Central. No structural model has, however, been proposed by these authors.

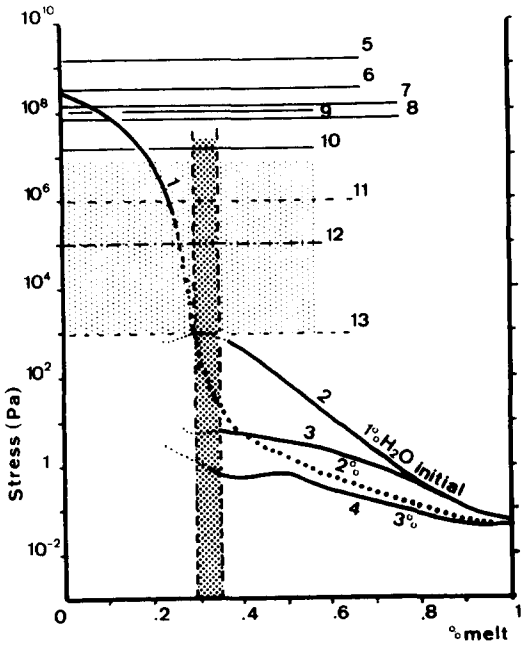


Fig. 18. Strength of partially melted granites and enclosing rocks. Curve 1 gives the results of experimental deformation of partially melted granites at a rate of $10^{-5}\,s^{-1}$ (van der Molen & Paterson 1979); Curves 2, 3 and 4 give the results of computation of the strength of suspension-like magmas with increasing crystallization from 10 kb and 1200°C to 2 kb and 650°C, for the studied granitoids, using Carron *et al.'s* (1978) program. Numbers on the curves indicate the initial water content of the magma used in computations. The strength has been calculated assuming a strain rate of $10^{-5}\,s^{-1}$. Curves 5 to 10 gives values for solid rocks similar to those constituting the envelope of the massif. Strain rates of $10^{-5}\,s^{-1}$ to $10^{-6}\,s^{-1}$. 5 and 6: Westerly granite, 700–900°C (Tullis & Yund 1977); 7 and 8: Biotite at respectively 400 and 600°C (Etheridge *et al.* 1973); 9 and 10; Synthetic phlogopite growing during deformation (Etheridge *et al.* 1974). The pale stippled field represents the range of strength the rising magma must have to be emplaced as mushroom or dome-like massifs from model experiments. Lines 11 and 12 assume an 'effective viscosity' ratio of $10^{-2}$ and $10^{-3}$ with mica rocks, which are likely to represent the actual enclosing rocks, and about $10^{-3}$ to $10^{-4}$ with granites. These viscosity ratios best correspond to those in model experiments. Line 13 assumes an 'effective viscosity' ratio of $10^{-4}$ with the most ductile phlogopite rocks. This 'viscosity ratio' is markedly lower than in model experiments and the corresponding 'strength' of the magma may be considered as the minimum strength. No maximum value of the 'effective viscosity' ratio being required, the upper limit of the field is only drawn for clarity. The dark stippled field represents the critical crystal content separating suspension-like behaviour (to the right) from granular framework-controlled behaviour (to the left), from van der Molen & Paterson's (1979) results.

Den Tex's (1975) and Talbot's (1974) model is, in outline compatible with the present observations. However, two additional factors may be considered:

(i) The uplift may have been induced by the density contrast between the largely anatectic base and the non-anatectic upper part of the mica-rich metasedimentary series. It can be shown from the calculations above, that 30 per cent melting of such mica-rich rocks would reduce the density by about 0.2 g $cm^{-3}$, which could be sufficient to create the gravitational instability (e.g. Ramberg 1979).

(ii) The characteristics and arrangement of metamorphic domes, their relationships with gneiss domes and plutonic massifs, and model experiments (see below), all suggest that they been caused by/or that they have developed together with, the diapiric emplacement of underlying gneiss domes or plutonic domes.

These interpretations do not contradict Den Tex's (1975) and Talbot's (1974, 1977) models. They have the advantage of accounting for the development of small-scale domes and their relationships with plutonic bodies.

The major domes may have been basically due to the uplift of granulitic gneiss domes, or possibly, in certain cases, directly to the diapiric rise of basic or ultrabasic material, also responsible for the passive doming of granulitic domes (see above and Fig. 24). Observations of ultrabasic intrusions contemporary to the development of regional metamorphism and deformation (e.g. Gavarnie dome, Moreau 1975), may support the feasibility of the latter interpretation.

Minor metamorphic-structural domes, occurring at higher structural levels, are likely to have been related to the uplift of synkinematic plutons as shown by their relationships with neighbouring plutonic massifs (e.g. Barousse dome, De Villechenous 1980) and the frequent intrusion of late-magmatic products in their central part.

On the map and structural reconstruction (Fig. 19), the domes have a concentric arrangement. Granulitic gneiss domes, or metamorphic domes, are situated at the centre; augen gneiss domes in a peripheral situation and granite massifs in a still more external position. This suggests that augen gneiss domes and plutonic domes are second-order domes with respect to metamorphic domes. This arrangement would, thus, represent a type of polydiapirism (Ramberg 1968, Stephansson 1974,

Stephansson & Johnson 1976) but with different origins for the constituent domes.

## STATE OF CRYSTALLIZATION OF THE GRANITIC MAGMAS AT THE TIME OF EMPLACEMENT

The similarity between plutonic domes and gneiss domes strongly suggests that the former were emplaced as highly crystallized magmas. This agrees well with the predictions of Ramberg, who showed from his model studies that a dome or a mushroom-like structure develops when there is only a small viscosity ratio between the rising body and its enclosing medium (e.g. Ramberg 1967, 1970).

Progress in the knowledge of the rheological properties of crystallizing magmas and the recent results of experimental deformation of partially melted granites by van der Molen & Paterson (1979) now enable us to estimate the crystal content of the magmas at the time of their emplacement.

In order to estimate the effective viscosity, and thus the strength, of the suspension-like magma, the program elaborated by Carron and Dujon (Carron *et al.* 1978) was applied to the granitoids in this study (Borrel & Soula, in preparation). The right hand curves in Fig. 18 represent the three possible values of initial water content as previously used for estimating the density of the magmas (2 and 3% are considered to have been the most likely, Borrel 1978). It should be noted that an increase in initial water content has the effect of producing a gentler slope in the curves, up to about 60% crystals.

The results of van der Molen & Paterson's (1979) experiments are shown on the same diagram. These results were obtained for a strain rate of $10^{-5}$ s$^{-1}$, and this value has been used in the calculation of the strength of the suspension-like magma. Taken together, these data show a sudden increase in the strength of the magma when the crystal content reaches about 70%, i.e. a value very close to the critical value separating suspension-like behaviour from framework controlled behaviour as predicted by van der Molen & Paterson (1979). Even through the experiments are preliminary ones (van der Molen & Paterson 1979), it is assumed that the general trend will not change, even if the point of maximum curvature varies slightly. It will be shown that changes of about $10^{-2}$ will not alter the result.

Figure 18 also shows from the literature the strength of rocks similar to those forming the host rocks of the massifs for similar strain rates (refs. in Fig. 18). These values are used in order to estimate effective viscosity contrasts (strength contrasts) between plutonic rocks and host rocks. Viscosity ratios required for the development of dome to mushroom-like structures in model studies cannot be less than $10^{-3}$ (may be $10^{-4}$) and can reach practically infinite values ('rigid' bodies intruding ductile overburden, Ramberg 1967, 1980). Values giving experimental structures closest to the observed structures are in general about $10^{-2}$. From Fig. 18 it can be shown that for such strength contrasts, the crystal content of the emplacing magmas must be greater than 70%. It should be noticed that for lower strain rates, such as those expected from geological data, the curves for the suspension-like behaviour will be displaced downwards and towards the left on the graph, showing a still gentler slope. The curves for low melt-fraction rocks will probably also be displaced downwards and to the left, but to a lesser extent, the behaviour being less sensitive to strain rate (van der Molen & Paterson 1979). Therefore, the change in strength will be likely to be still more marked for the critical crystal content. As the strength of the host-rocks is similarly less sensitive to strain rate (see refs. in Fig. 18), the strength contrast between magma and enclosing rocks will be emphasized still further.

## ROLE OF DIFFERENCES IN VISCOSITY IN SIMULTANEOUS UPLIFT OF DIFFERENT BODIES

Field data and theoretical arguments strongly suggest that differences in behaviour between the different types of domes and their relationships with each other are related to small differences in the viscosity of the rising bodies. Special centrifuge models were built in order to clarify this aspect. Some more elaborate models were then constructed in order to better simulate the actual field structures.

### *First series of model experiments*

Two types of source layers were used, one with a smaller density (1.1 g cm$^{-3}$) and a greater viscosity, the other with a greater density (1.15 g cm$^{-3}$) and a smaller viscosity. The viscosity ratio between the source layer and its cover was about 10–20. The first type of source layer was aimed at representing less dense (more acidic) but stronger gneisses, the second, denser but less viscous plutonic granitoids (with average composition of granodiorite).

In the first models (Figs. 20a & b) one block of each of the two types of potential diapiric materials was emplaced at the base of a single model, at the same depth in each model, under a layered sequence representing the metasedimentary series. At the end of the experiments, only the less viscous body (granite) had risen, despite its greater density (Fig. 21a). In order to induce the two bodies to rise to the same height, it was found necessary to place the more viscous body at higher levels initially (Fig. 21b). This can explain how denser plutonic rocks, initially situated at deeper levels may have been intruded at higher levels in the crust than the gneisses. If the less viscous rocks (or magmas) are at the same time the lighter, the uplift is likely to be still more rapid with respect to the more viscous (and denser) rocks, that is, for lighter magmas to be emplaced at the same height as solid gneisses they must have been generated (or stored) at still deeper levels. Incidentally, this favours the hypothesis that the granitoids were derived from deep-

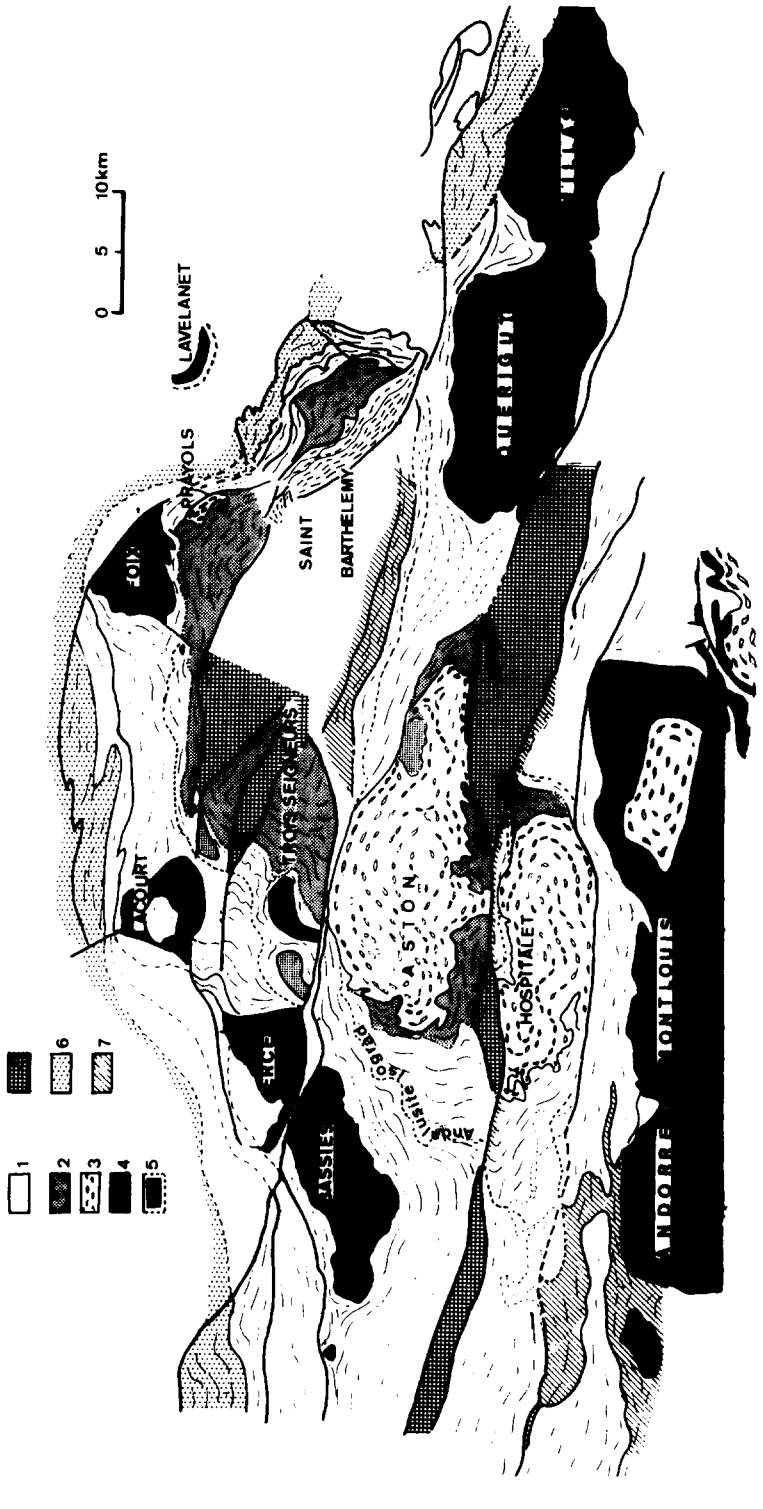


Fig. 19. Restoration of the pre-Alpine structure by reciprocal displacement along the major Alpine faults. The gaps in the restoration (cross-hatched) are due to the impossibility of unfolding the cartographic Alpine folds and fold-bands. (1) Pre-Silurian metasedimentary rocks; (2) areas of migmatization (metasediments and augen gneisses); (3) augen gneisses; (4) plutonic rocks; (5) Lavelanet granodiorite (recognized by drilling); (6) nodular limestone ('calcaire griotte') facies in the Upper Devonian; (7) low-contrast facies in the Upper Devonian.

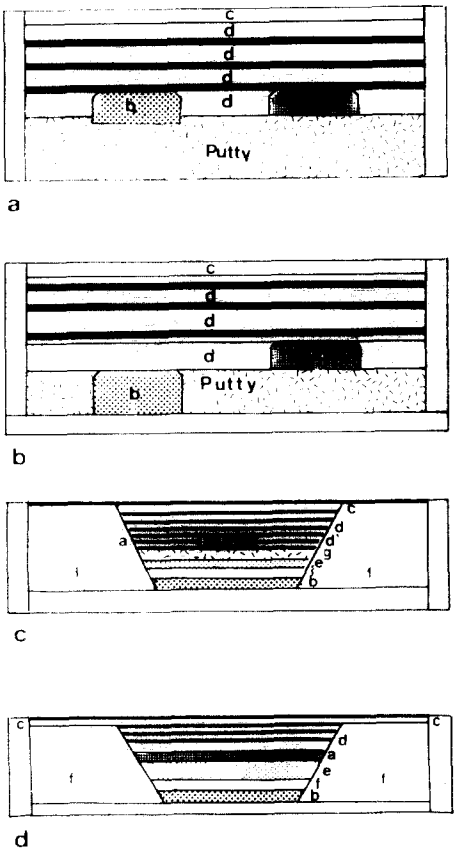


Fig. 20. Initial construction of the models before centrifuging. From the (a) to (d), initial configurations for models in Figs. 22(a) & (b), 23 and 24. (a) medium 'viscosity' silicon putty with density 1.1 g cm$^{-3}$ (representing the gneisses); (b) low 'viscosity' silicon putty with density 1.15 g cm$^{-3}$ (simulating the granitoids); (c) medium 'viscosity' silicone putty with density 1.1 g cm$^{-3}$; (d) medium 'viscosity' silicone putty with density 1.25 g cm$^{-3}$; (e) high 'viscosity' silicone putty with density 1.57 g cm$^{-3}$; (f) high 'viscosity' silicone putty with density 1.25 g cm$^{-3}$; (g) plastic base putty with density 1.9 g cm$^{-3}$.

seated magmas, as proposed by Marre (1973) and Borrel (1978). Moreover, it should be stressed that only the last stage of the ascent, when the magma was richer in crystals, i.e. the emplacement, was considered in these experiments, and that the first stage of the ascent of the magma with its low crystal content, is likely to have been much more rapid (Ramberg 1967, 1970).

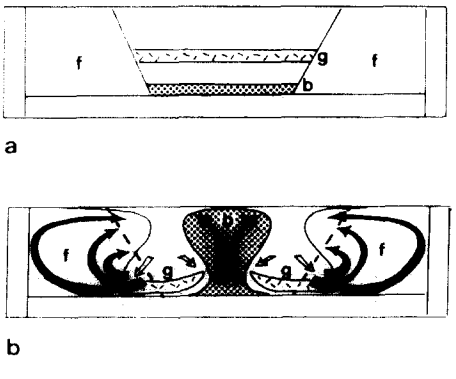


Fig. 22. Schematic evolution of centrifuged models with initially oblique walls. (a) Initial state; (b) Model after centrifuging. The compression develops as a result of upward and centripetal migration of the wall-forming material (see Figs. 20c & d). Black arrows indicate the displacement path of the wall-forming material as followed by bulbs and impurities trajectories; white arrows indicate the displacement path of the densest material.

*Second series of model experiments*

More elaborate models were built in order to represent as closely as possible the initial structure of the region. These models were constructed in such a way that lateral compression occurred during diapirism. This compression was induced by a centripetal movement of the less dense walls of the 'useful' central part of the models, initially inclined at about 30° to the vertical (Fig. 21). As shown in Figs. 22 and 23 lateral shortening decreases from the upper part to the base of the models, and it has not been possible to model homogeneous lateral shortening. However, such a shortening may represent shortening related to, or accompanying, crustal overthrusting, and it may be questioned whether such a mechanism is not, in many cases, a more realistic geodynamic process than homogeneous lateral shortening.

In these models, the material representing less viscous and denser plutonic rocks was initially situated at the base of each model. The material simulating more viscous and lighter gneisses was initially situated above, immediately under an upper layered sequence, as in the Pyrenees the gneisses were probably below the pre-Silurian metasedimentary series. In the first type of model the lowest buoyant material represents granitic magma (layer b in Figs. 20c and 23), when it was at a late stage in its evolution and had a high crystal content. In the second type of model (Figs. 20d and 24), it could equally well represent ultrabasic material coming from partial melting of the upper mantle (see earlier discussion).

In the first type of model, the upper layered series was modelled with a relatively low competency and in the second series of models its base was more competent.

The results of centrifuging these two types of model are shown in Figs. 23 and 24.

In the first type of model, the 'gneisses' show a dome-like structure and the 'granites' a mushroom-like structure (Fig. 23). The most striking feature of these models is the interpenetrating rise of the two types of material. Depending on the model, the gneisses form the core of the composite structure, surrounded by the granite, or are situated at the periphery and seem to be intruded by the granite.

In the second type of model, the rise of buoyant material induced a passive doming of the layered series. Two cases may be distinguished: (1) when the basal competent strata were continuous, they stopped the rising material and a dome structure developed with a well arched shape (Fig. 24a) and (2) when a vertical or steeply inclined discontinuity was inserted in the competent strata, the rising material rose through it and spread out into a mushroom-shaped diapir above (Fig. 24b).

It should be noticed that in both series of models, buoyant material can intrude lighter overburdens (e.g. buoyant material with density 1.15 g cm$^{-3}$ intruding overburden with density 1.1 g cm$^{-3}$). This situation was also observed in the field where granitic, granodioritic or basic plutonic bodies intrude, for example sandstone

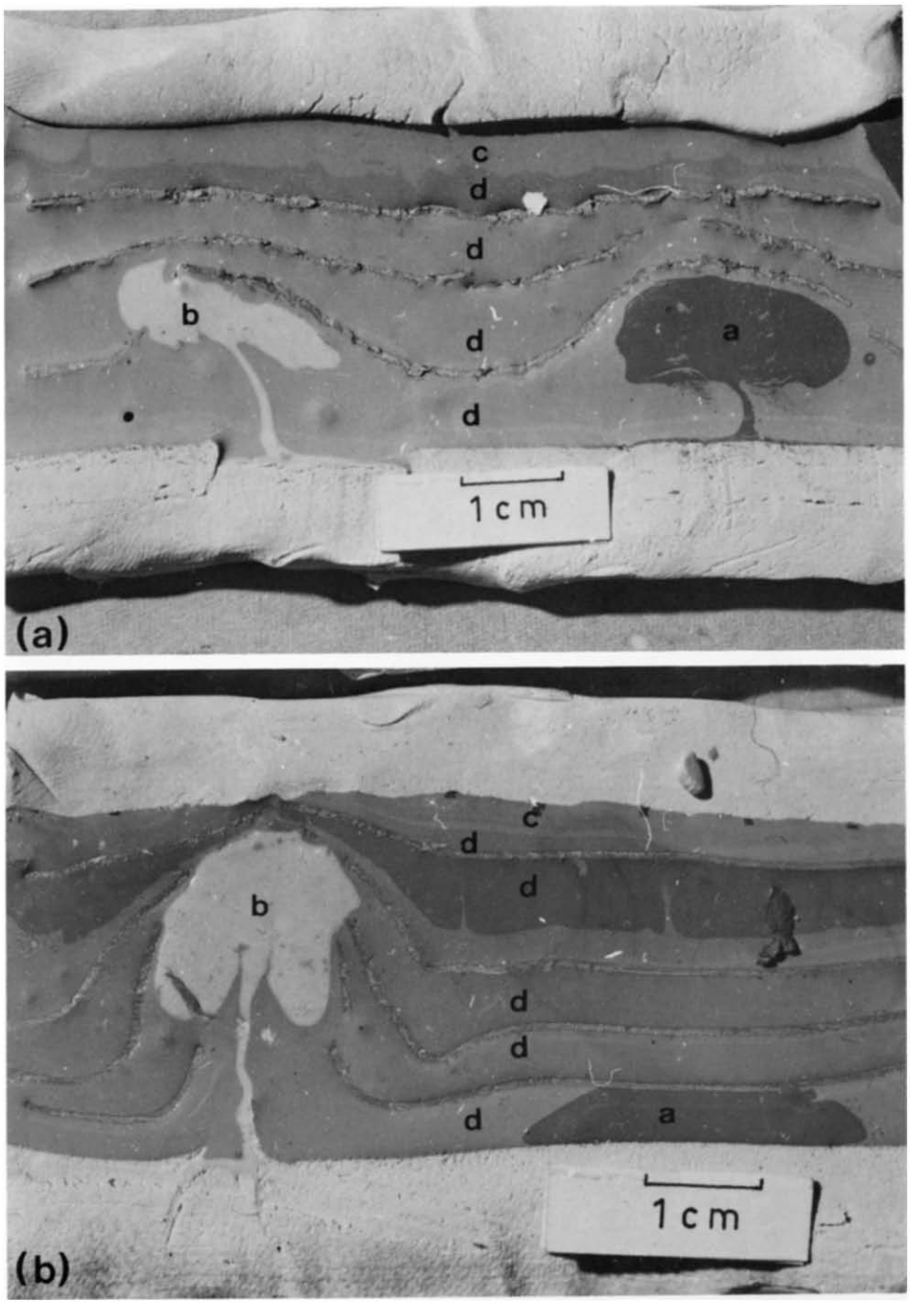


Fig. 21. Centrifuge experiments with no compression in the central part. (a) Two blocks of silicone with different density and viscosity initially disposed at the same level (see Fig. 20a). After centrifuging, only the less viscous block has been uplifted in spite of its greater density. Note the pear-like shape of the dome. (b) The lighter but more viscous block was disposed at a higher level than the denser but less viscous block in the stratigraphic pile (see Fig. 20, second model from the top). The two domes attained the same level when centrifuging was stopped.

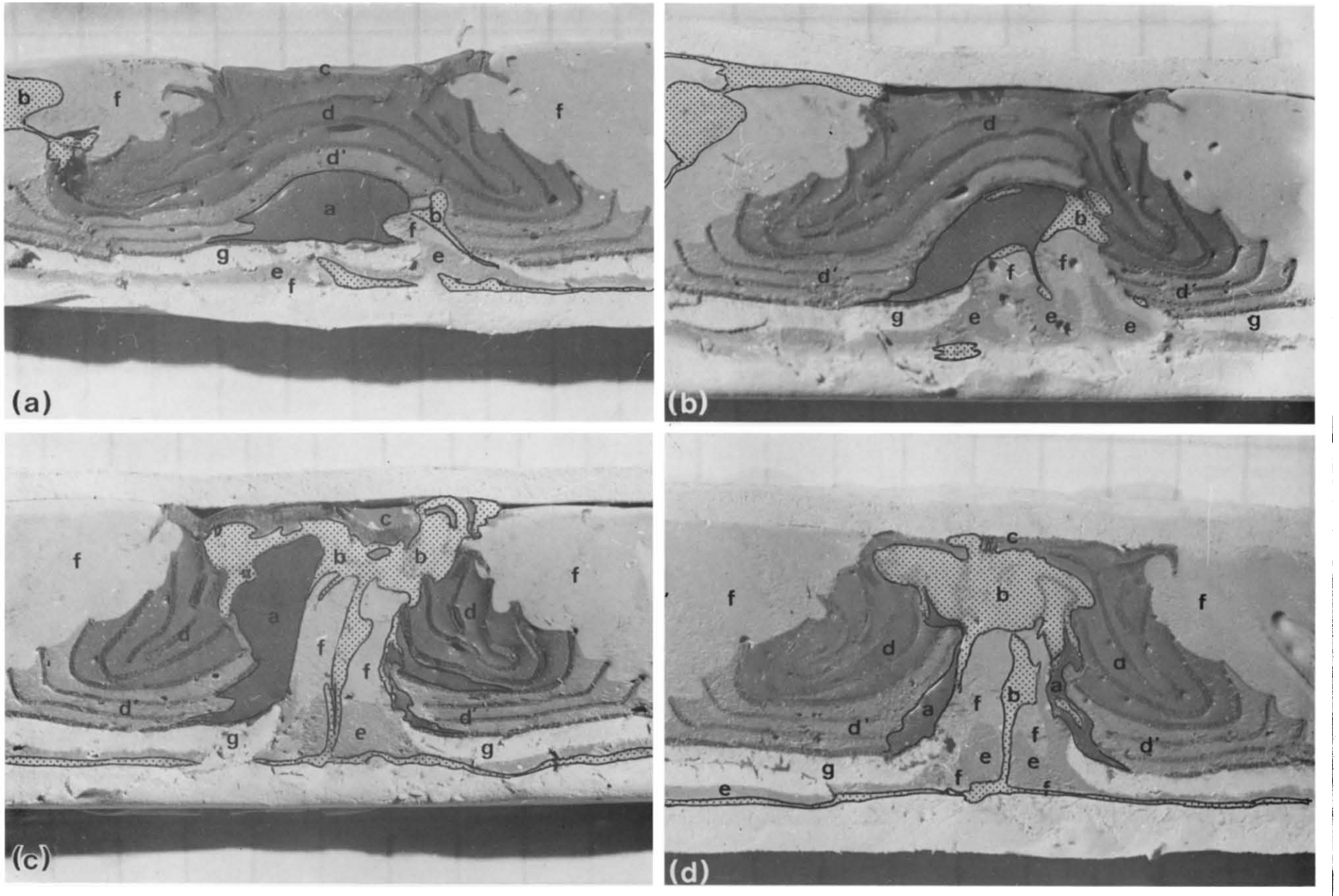


Fig. 23. Diapirism with compression in the central part of the model (see Fig. 22). The lighter but more viscous material was initially situated at a higher level than the denser but less viscous layer (see Fig. 20c.). The 'stratigraphic' pile above the upper bouyant layer was made of a low competency. (a), (b), (c) and (d) are serial cross-sections in a same model, showing the possible variations in the apparent relationships between two rising bodies with different properties in the same 'regional' structure. In (a) and (b), the more superficial and stronger material ('the gneisses') made up a rounded-shaped dome and the deeper and more ductile material (the 'granite') intruded along the discontinuities at the interface between the dome and the envelope. In (c) and (d), the stronger material is pulled up and intruded by the less viscous material (the 'granite') which rose faster.

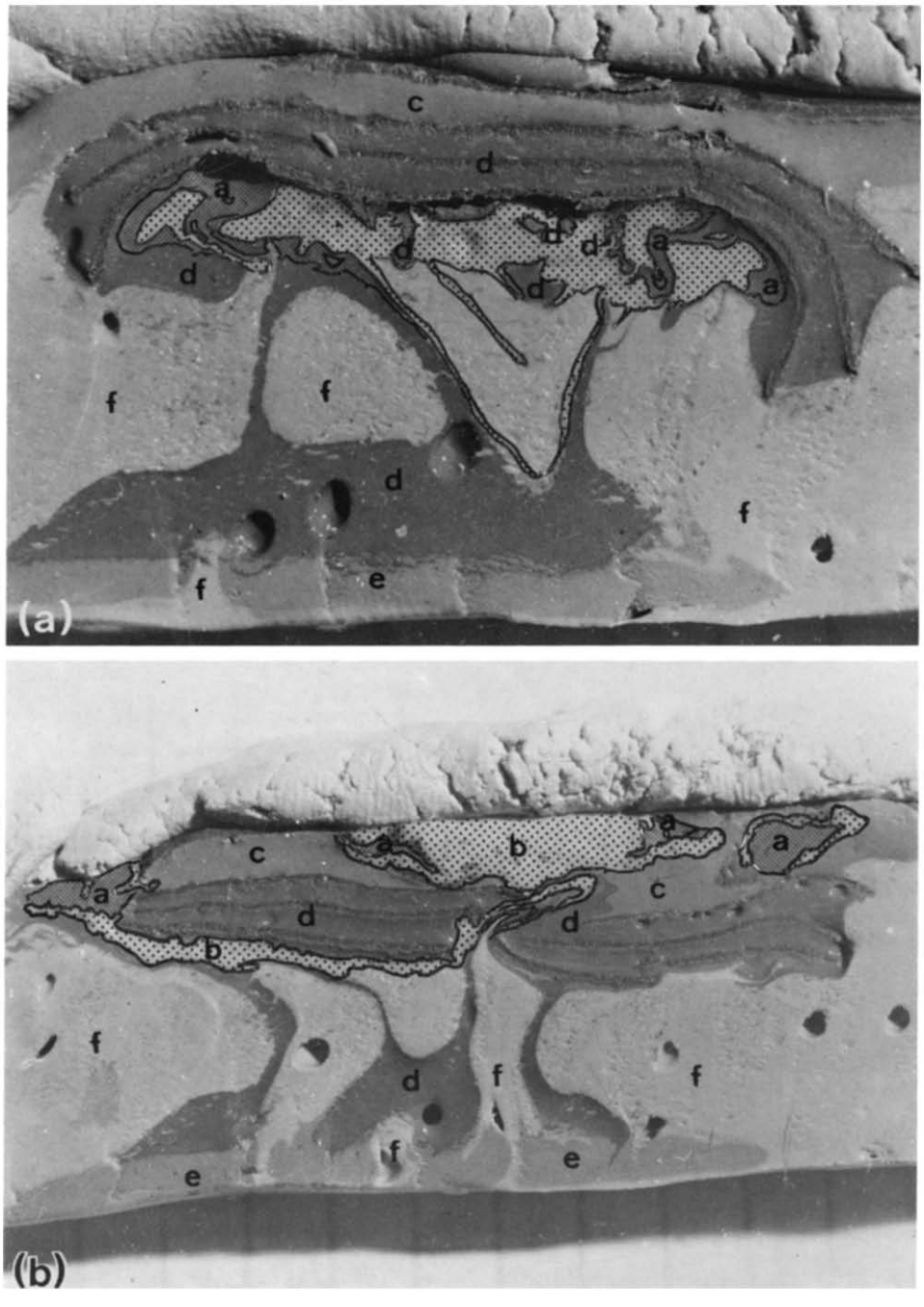


Fig. 24. Diapirism with compression in the central part of the model (see Fig. 21). Same type of model as Fig. 23 (model d in Fig. 20). The upper stratigraphic pile was made more competent than in Fig. 23 by introduction of thicker plasticine layers at its base. (a) No discontinuity in the upper stratigraphic pile. This upper series has gained a dome shape by being pulled up by rising material. (b) Same type of model as in (a) but with an initial vertical discontinuity in the competent upper series. The rising material passes across the competent layers through this vertical fracture and develops a mushroom-like structure above by lateral expansion in lighter material situated in the uppermost part of the series.

deposits, and has also been obtained experimentally by Ramberg (1967).

The structures obtained in the present model experiments are similar to those observed in the field, and in some instances, offer alternative explanations to the interpretations usually proposed.

The first type of model shows structures similar to those observed in the plutonic massifs and the augen gneisses. Both situations shown in Fig. 23 are commonly seen in the field: the augen gneisses are commonly surrounded by granites as simulated in Figs. 23 (a) and (b), as for example, in the eastern part of the Andorre–Montlouis granite (see Fig. 3). Conversely, the granites are often seen occurring inside gneiss massifs as illustrated in Figs. 23 (c) & (d). This is the case for the Costabonne granite in the nearby Canigou augen gneiss massif (e.g. maps by Autran *et al.* 1970 or Zwart 1972). These situations have been interpreted differently by those authors, who considered that the intrusion of the granites post-dated the doming. The models show that this is not necessarily true, and that the criterion of apparent cross-cutting may not be diagnostic of time emplacement relationships but of relative behaviour of the different types of rising materials (doming materials) with different viscosities (strengths).

In these models, viscosity appears to have played a prominent role in controlling the rate and geometry of uplift of the various rising bodies, but this control applies only to materials having similar composition and density. It should be noted, however, that in Ramberg's (1967, 1970) models, very low viscosity materials, i.e. water simulating liquid magmas, show a very rapid rate of rise.

The second type of model exhibits structures which seem rather similar to those of granulitic gneiss domes. This seems to favour the hypothesis of the passive doming of the gneisses, induced by the rise of underlying ultrabasic magmas.

## CONCLUSIONS AND FURTHER CONSEQUENCES

The observations and model studies lead to a general interpretation of gneissic, plutonic and metamorphic domes as due to diapirism during major regional shortening.

The various relationships between the different kinds of domes are attributed to the nature of the rising material, to differences in density, but also to differences in viscosity. Different types of cross-cutting relationships may be attributed to differences in behaviour of various materials during their simultaneous uplift, i.e. to differences in uplift rate and in competency.

The granitoid magmas may be shown to have been emplaced at their present level within the Palaeozoic rocks in a highly crystallized state, with more than 70% crystals. This does not imply that the rise took place entirely with such a high crystal content. At this critical value, theory and experiment demonstrate that the strength suddenly changes, and becomes much larger with a small increase in crystal content. The rate and mode of uplift will be considerably modified at this stage, becoming a classical diapiric type similar to mantled gneiss domes. Therefore, uplift will be controlled by the last crystallizing minerals.

The granulitic gneiss domes and the metamorphic domes may have been due to passive doming in response to the rise of magmas generated at depth, possibly derived from partial melting of the upper mantle.

Thermal domes are thought to derive from the diapiric uplift of gneiss domes and plutonic domes. Some, however, may have been due directly to the rise of ultrabasic magmas.

As this composite diapirism occurred on different scales during regional shortening, the question of the origin of this regional shortening arises. Is this shortening due to crustal shortening (e.g. plate motion) or related to gravitational instability of the lower crust, as suggested by Ramberg & Sjöström (1973)? No structural evidence offers an obvious solution to this problem. It should be noted that, according to Vitrac-Michard *et al.* (1980), the hypothesis of subduction may be rejected for the Hercynian orogen, and a regional deep-seated gravitational instability is envisaged as triggering the metamorphic–plutonic process in the model they propose. In any event, when considering the cause of regional shortening, the possibility of a deep-seated gravitational instability must not be rejected out of hand.

Whatever the cause of regional shortening, diapirism is believed to have played a prominent role in controlling the structure and the metamorphism during the Hercynian orogenesis. This Hercynian diapirism is also believed to have played an important role in controlling the post-Hercynian (Alpine) evolution of the orogen (Soula 1979, Soula & Bessière 1980).

Evidence of diapirism of gneisses, plutonic rocks and metamorphic rocks is common in many orogenic belts. In the Hercynian orogenic belt, such evidence of diapirism has been found in zones other than the Pyrenees (e.g. Den Tex 1975, Brun 1975, Audren 1976, Ledru & Brun 1977, Hanmer & Vigneresse 1980, Couturier & Didier 1980).

These diapiric events have usually been considered independently of each other, or from the other structural, metamorphic or plutonic events. From the present results, it is probable that many of these structural, metamorphic and plutonic events were inter-related, apparent geometrical cross-cutting or even apparent superposition relationships being due to differences in competency, linked to differences in the physical and rheological properties of the various materials which rose at different rates.

*Acknowledgements* — Centrifuge experiments were performed at the Tectonic Laboratory of the Institute of Geology of the University of Uppsala (Sweden) and I would like to thank H. Ramberg, R. Hâll and H. Sjöström for their help and suggestions during this work. The study on viscosity and density of crystallizing granites was carried out in collaboration with A. Borrel and special thanks are due to J. P. Carron

and St. Cl. Dujon for providing their unpublished program and for their help in using it. I am also grateful to D. Elliott, M. Lelubre, J. Martignole, J. G. Ramsay and P. Sirieys for stimulating discussions and to the editor Dr. A. J. Barber and an anonymous referee of the J. S. G. for their constructive comments. M. Aparicio, J. Déramond, P. Debat and J. Y. Guchereau participated at various stages of the investigation. R. H. Graham reviewed the final form of the English text.

## REFERENCES

Albarède, F. 1976. Thermal models of post-tectonic decompression as exemplified by the Haut-Allier granulites (Massif Central, France). *Bull. Soc. géol. Fr.* **18,** 1023–1032.

Aparicio, M. 1975. métamorphisme et déformation au contact d'un massif plutonique: l'encaissant du complexe de Querigut. Thèse 3ème cycle, Toulouse.

Aparicio, M., Déramond, J. & Soula, J. C. 1975. Mouvements hercyniens tardi-métamorphiques dans la zone de la faille Nord-Pyrénéenne ariégeoise. *3ème Réun. A. Sci. Terre,* Montpellier, 14.

Aparicio, M. & Lelubre, M. 1976. Les kink-bands de l'encaissant du Querigut: exemple de détermination géométrique de l'orientation du tenseur des contraintes. *Bull. Soc. géol. Fr.* **6,** 1511–1514.

Audren, C. 1976. Modèle de la mise en place des massifs anatectiques en Bretagne méridionale. *4ème Réun. A. Sci. Terre*, Rennes, 23.

Autran, A., Fonteilles, M. & Guitard, G. 1966. Discordence du Paléozoïque inférieur sur un socle gneissique antecambrien dans le massif des Albères (Pyrénées Orientales). *C. r. hebd. Séanc. Sci., Paris* **D263** 317–320.

Autran, A. Fonteilles, M. & Guitard, G. 1970. Relations entre les intrusions de granitoïdes, l'anatexie et le métamorphisme régional considérés principalement du point de vue du rôle de l'eau. *Bull. Soc. géol. Fr.* **4,** 673–731.

Barrouquère, G. 1968. Structure des formations paléozoïques du massif de l'Arize (Pyrénées ariégeoises). *Bull. Bur. Rech. géol. min.* Fr. Sect. 1, **4,** 1–10.

Barrouquère, G. Castaing, C. & Roux, L. 1976. Carte géologique de Saint-Girons; Terrains ante-hercyniens. Carte Géologique de la France au 1/50 000, B.R.G.M.

Berger, A. R. & Pitcher, W. S. 1970. Structure in granitic rocks; a commentary and a critique on granite tectonics. *Proc. geol. Ass.* **81,** 441–461.

Berner, H. Ramberg, H. & Stephansson, O. 1972. Diapirism in theory and experiments. *Tectonophysics* **14,** 197–218.

Birch, F. 1966. Compressibility; elastic constants. In: *Handbook of Physical Constants, revised edition* (edited by Clark, S. D., Jr.) *Mem. geol. Soc. Am.* **97,** 97–174.

Borrel, A. 1978. Le massif granitique du Sidobre: petrographique, structure, relations mise en place- cristallisation. Thèse 3ème Cycle, Toulouse.

Brun, J. P. 1975. Contribution à l'étude d'un dôme gneissique: le massif de Saint-Malo; analyse de la déformation. Thèse 3ème Cycle, Rennes.

Brun, J. P. 1980. The cluster ridge pattern of mantled gneiss domes in eastern Finland: evidence for large scale gravitational instability in the Proterozoïc crust. *Earth Planet. Sci. Lett.* **47,** 441–449.

Brun, J. P. & Pons, J. 1981. Strain patterns of pluton emplacement in a crust undergoing non coaxial deformation. *J. Struct. Geol.* **3,** 219–229.

Carron, J. P., Dujon, S. Cl. & Jonin, M. 1978. A propos des enclaves de la granodiorite de Vire: quelques indications préliminaries sur l'évolution des propriétés physiques des magmas granitiques au cours de leur cristallisation. *Bull. Soc. géol. Fr.* **20,** 739–744.

Castaing, C. 1972. Microtectonique de l'Arize centrale métamorphique (Pyrénées ariégeoises). Thèse 3ème Cycle, Toulouse.

Castaing, C., Roux, L. & Soula, J. C. 1973. Métamorphisme dans les massifs de l'Arize et des Trois Seigneurs (Pyrénées ariégeoises). *1ère Réun. A. Sci. Terre,* Paris, 121.

Clin, M. 1964. Etude géologique de la haute chaine des Pyrénées centrales entre le cirque de Troumouse et le cirque du Lys. *Mem. Bur. Rech. géol. min. Fr.* **27,** 1–379.

Cobbold, P. J. & Quinquis, H. 1980. Development of sheath folds in shear regimes. *J. Struct. Geol.* **2,** 119–126.

Cooper, M. A. & Bradshaw, R. 1980. The significance of basement gneiss domes in the tectonic evolution of the Salta Region, Norway. *J. geol. Soc. Lond.* **137,** 231–240.

Couturier, J. P. & Didier, J. 1980. Quelques effets de la montée diapirique du complexe granitique du Velay. *8ème Réun. A. Sci. Terre,* Marseille, 112.

Daly, R. A., Manger, G. E. & Clark, S. P., Jr. 1966. Density of rocks. In: *Handbook of Physical Constants, revised edition* (edited by Clark, S. P., Jr.) *Mem. Geol. Soc. Am.* **97,** 19–26.

Debat, P., Sirieys, P., Deramond, J. & Soula, J. C. 1975. Paleo-déformation d'un massif orthogneissique. *Tectonophysics* **28,** 159–183.

Debat, P., Soula, J. C., Kubin, L. & Vidal, J. L. 1978. Optical studies of natural deformation structures on feldspars from Occitania (Southern France). *Lithos* **11,** 133–145.

Debon, F. 1975. Les massifs granitoids à structure concentrique de Cauterêt-Panticosa (Pyrénées Occidentales) et leurs enclaves. *Sciences Terre,* Mem. 33.

Den Tex, E. 1975. Thermally mantled gneiss domes: the case for convective heat flow in more or less solid orogenic basement. In: *Progress in Geodynamics* (edited by Borradaile, G. J., Ritsema, A. R., Rondeel, H. E. & Simon, O. J.) North Holland Publishers, Amsterdam, 62–79.

Déramond, J. 1971. Plis couchés dans la zone axiale des Pyrénées ariégeoises (Haut Salat). *C. r. hebd. Séanc. Acad. Sci., Paris* **D272,** 693–696.

Déramond, J. Mangin, A., Roux, L. & Soula, J. C. 1969. Déformations superposées et figures d'interférence dans les Pyrénées ariégeoises. *C. r. hebd. Séanc. Acad. Sci., Paris* **D269,** 2309–2313.

Déramond, J., Mirouse, R. & Soula, J. C. 1971. Déformations hercyniennes superposées dans la vallée de la Valira del Oriente (Pyrénées andorranes). *C. r. somm. Séanc. Soc. géol. Fr.* 123–124.

De Villechenous, F. 1980. Géologie de la partie occidentale du massif varisque de la Barousse (Pyrénées centrales). Thèse 3ème Cycle, Toulouse.

Dixon, J. M. 1975. Finite strain and progressive deformation in models of diapiric structures. *Tectonophysics* **28,** 89–124.

Elder, J. W. 1970. Quantitative laboratory studies of dynamical models of igneous intrusions. In: *Mechanisms of Igneous Intrusion* (edited by Newall, G. & Rast, N.) *Geol. J. Spec. Issue* **2,** 245–260.

El Hourani, H. 1980. Les roches basiques métamorphisées du massif de Castillon (Pyrénées ariégeoises) Thèse 3ème Cycle, Toulouse.

Etheridge, M. A., Hobbs, B. E. & Paterson, M. S. 1973. Experimental deformation of single crystals of biotite. *Contr. Miner. Petrol.* **38,** 21–36.

Etheridge, M. A. Paterson, M. S. & Hobbs, B. E. 1974. Experimentally produced preferred orientation in synthetic mica aggregates. *Contr. Miner. Petrol.* **44,** 275–294.

Fletcher, R. C. 1972. A finite-amplitude model for the emplacement of mantled gneiss domes. *Am. J. Sci.* **272,** 197–216.

Fonteilles, M. 1976. Essai d'interprétation des compositions chimiques des roches d'origine métamorphique et magmatique du massif hercynien de l'Agly (Pyrénées Orientales). Thèse Sciences, Paris VI.

Fonteilles, M. & Guitard, G. 1974. Influence des noyaux de socle précambriens sur le métamorphisme et la structure profonde de l'orogénèse hercynienne des Pyrénées. Comparison avec les régions voisines. *1° I.C.G., Précambrien des Zones Mobiles de l'Europe, Conférence Liblice,* 1972, Praha, 189–198.

Fyson, W. K. & Fryth, R. A. 1979. Regional deformations and emplacement of granitoid plutons in the Heckett River greenstone belt, Slave Province, Northwest Territories. *Can. J. Earth Sci.* **16,** 1187–1195.

Guchereau, J. Y. 1975. Le Saint Barthélémy métamorphique. Thèse 3ème Cycle, Toulouse.

Guitard, G. 1970. Le métamorphisme hercynien mesozonal et les gneiss oeillés du massif du Canigou (Pyrénées Orientales). *Mem. Bur. Rech. géol. min. Fr.* **63.**

Guitard, G. 1976. Aspects des relations entre tectonique et métamorphisme. *Bull. Bur. rech. géol. min. Fr.* (I), **4,** 325–341.

Guitard, G. 1977. Aperçu sur la géologie de la chaine hercynienne des Pyrénées orientales entre le Salat et la Méditerranée. In: *Guides Géologiques Régionaux de la France: Pyrénées Orientales, Corbières* (edited by Jaffrezo, M.) Masson, Paris, 9–21.

Hanmer, S. & Vigneresse, J. L. 1980. Mise en place des diapirs synectoniques dans la chaine hercynienne: exemple des massifs leucogranitiques de Locronan et de Pontivy (Bretagne Centrale). *Bull. Soc. géol. Fr.* **22,** 193–202.

Hudleston, P. J. 1973. Fold morphology and some geometrical im-

plications of theories of fold development. *Tectonophysics* **16,** 1–46.
Jaeger, E. & Zwart, H. J. 1968. Rb–Sr age determination of some gneisses and granites of the Aston–Hospitalet massif (Pyrenees). *Geologie Mijnb.* **47,** 349–357.
Laffont, D. 1971. Le massif granitique de Querigut-Millas entre Roquefort de Sault et Mosset. Thèse 3ème Cycle, Toulouse.
Lamouroux, C. 1976. Les mylonites dans le massif de Néouvielle. Thèse 3ème Cycle, Toulouse.
Lamouroux, C., Soula, J. C., Déramond, J. & Debat, P. 1980. Shear zones in the granodioritic massifs of the Central Pyrenees and the behaviour of these massifs during the Alpine orogenesis. *J. Struct. Geol.* **2,** 49–53.
Lamouroux, C., Soula, J. C. & Roddaz, B. 1981. Les zones mylonitiques des massifs de Bassies et de l'Aston (Haute Ariège). *Bull. Bur. Rech. géol. min. Fr.* **2,** 103–111.
Ledru, P. & Brun, J. P. 1977. Utilisation des fronts et trajectoires de schistosité dans l'étude des relations entre tectonique et intrusions granitiques: exemple du granite de Flamanville (Manche). *C. r. hebd. Séanc. Acad. Sci., Paris* **D285,** 1199–1202.
Lelubre, M. 1964. Existence d'un socle probablement précambrien dans la région de Bompas-Arnave (Ariège). *C. r. hebd. Séanc. Acad. Sci., Paris* **D258,** 1272–1274.
Leterrier, M. 1972. Etude petrographique et géochimique du massif granitique de Querigut (Ariège). Thèse Sciences, Nancy.
Mangin, A. 1967. Etude géologique de la partie septentrionale du massif du Saint-Barthélémy (Pyrénées ariégeoises). Thèse 3ème Cycle, Toulouse.
Marre, J. 1973. Le complexe éruptif de Querigut. Pétrologie, structurologie, cinématique de mise en place. Thèse Sciences, Toulouse.
Martignole, J. 1964. Recherches pétrographiques et structurales dans la région d'Ax les Thermes. Thèse 3ème Cycle, Toulouse.
Martignole, J. & Schrijver, K. 1970a. Tectonic setting and evolution of the Morin anorthosite, Greenville Province, Quebec. *Bull. geol. Soc. Finl.* **42,** 165–209.
Martignole, J. & Schrijver, K. 1970b. The level of anorthosites and its tectonics pattern. *Tectonophysics* **10,** 403–410.
Martignole, J. & Schrijver, K. 1977. Anorthosite–Farsundite complexes in the Southern part of the Greenville Province. *Geosci. Can.* **4,** 137–143.
Molen, I. van der, & Paterson, M. S. 1979. Experimental deformation of partially melted granite. *Contr. Miner. Petrol.* **70,** 299–318.
Mirouse, R. 1977. Paléozoïque supérieur et orogénèse varisque dans le domaine pyrénéen. In: *La Chaine Varisque d'Europe Moyenne et Occidentale*, Colloque International C.N.R.S., Rennes, no. 243, 559–569.
Moreau, C. 1975. L'enclave à staurotide-gedrite de la vallée d'Héas (Hautes Pyrénées) et son encaissant. Thèse 3ème Cycle, Toulouse.
Passchier, C. W. 1980. Deformation mechanisms in mylonite bands from the Saint Barthelemy massif. *Int. Conf. on the Effects of Deformation on Rocks*, Göttingen (abstracts), 201–202.
Pitcher, W. S. 1979. The nature, ascent and emplacement of granite magmas. *J. Geol. Soc. Lond.* **136,** 621–622.
Pons, J. 1971. Pétrofabrique et structures dans le massif de Querigut. Thèse 3ème Cycle, Toulouse.
Ramberg, H. 1967. *Gravity Deformation and the Earth's Crust.* Academic Press, London.
Ramberg, H. 1968. Instability of layered systems in the field of gravity. *Phys. Earth Planet. Interiors* **1,** 427–447.
Ramberg, H. 1970. Model studies in relation to intrusion of plutonic bodies In: *Mechanisms of Igneous Intrusion* (edited by Newall, G. & Rast, N.) *Geol. J.* **2,** 261–286.
Ramberg, H. 1972. Theoretical models of density stratification and diapirism in the Earth. *J. geophys. Res.* **77,** 877–889.
Ramberg, H. 1980. Diapirism and gravity collapse in the Scandinavian Caledonides. *J. geol. Soc. Lond.* **137,** 261–270.
Ramberg, H. & Sjöström, H. 1973. Experimental geodynamical models related to continental drift and orogenesis. *Tectonophysics* **19,** 105–132.
Ramsay, J. G. 1967. *Folding and Fracturing of Rocks.* McGraw-Hill, New York.
Robie, R. A., Bethke, P. M., Toulmin, M. S. & Edwards, J. L. 1966. X-ray crystallographic data, density, and molar volumes of minerals. In: *Handbook of Physical Constants* (edited by Clark, S. P., Jr.). *Mem. geol. Soc. Am.* **97,** 27–74.
Robin, P. Y. 1979. Theory of metamorphic segregation and related processes. *Geochim. cosmochim. Acta* **43,** 1587–1500.
Roux, L. 1968. Polymétamorphisme dans le massif de Castillon (Ariège). *C. r. hebd. Séanc. Acad. Sci., Paris* **266,** 752–754.
Roux, L. 1977. L'évolution des roches du facies granulite et le problème des ultramafitites dans le massif de Castillon (Ariège). Thèse Sciences, Toulouse.
Schwerdtner, W. M. & Tröng, B. 1978. Strain distribution within arcuate diapiric ridges of silicone putty. *Tectonophysics* **50,** 13–28.
Schwerdtner, W. M., Sutcliffe, R. H. & Tröng, B. 1978. Patterns of total strain in the crestal region of immature diapirs. *Can. J. Earth Sci.* **15,** 1437–1447.
Séguret, M. & Proust, F. 1968a. Contribution à l'étude des tectoniques superposées dans la chaine hercynienne: l'allure anticlinale de la schistosité à l'Ouest du massif de l'Aston (Pyrénées Centrales) n'est pas originelle mais due à un replissement. *C. r. hebd. Séanc. Acad. Sci., Paris* **D266,** 317–320.
Seguret, M. & Proust, F. 1968b. Tectonique hercynienne dans les Pyrénées Centrales: signification des schistosités redressées, chronologie des déformations. *C. r. hebd. Séanc Acad. Sci., Paris* **D266,** 984–987.
Skinner, B. J. 1966.Thermal expansion. In: *Handbook of Phyisical Constants* (edited by Clark, S. P., Jr.) *Mem. geol. Soc. Am.* **97,** 75–96.
Soula, J. C. 1969. Evolution structure de l'Arize orientale. Thèse 3ème Cycle, Toulouse.
Soula, J. C. 1970. Métamorphisme de contact et métamorphisme régional dans l'Arize orientale. *C. r. hebd. Séanc. Acad. Sci., Paris* **D270,** 1447–1450.
Soula, J. C. 1971. Evolution des structures hercyniennes de l'Arize métamorphique (Pyrénées ariègeoises). *Revue Géor. phys. Géol. dyn.* 2, XIII, **3,** 233–244.
Soula, J. C. 1979. Déformations hercyniennes et alpines dans les Pyrénées ariègeoises. Thèse Sciences, Toulouse.
Soula, J. C. & Bessière, G. 1980. Sinistral horizontal shearing as a dominant process of deformation in the Alpine Pyrenees. *J. Struct. Geol.* **2,** 69–74.
Soula, J. C. & Borrel, A. 1980. Controle de la densité et de la viscosité sur la mise en place des intrusions plutoniques. Signification de la forme et de la structure des massifs granitoïdes. *8ème Réun. A. Sci. Terre*, Marseille.
Soula, J. C. & Debat, P. 1976. Développement et caractères des litages tectoniques. *Bull. Soc. géol. Fr.* **18,** 1515–1537.
Stephansson, O. 1974. Polydiapirism of granitic rocks in the Svecofennian of Central Sweden. *Precambrian Res.* **2,** 189–212.
Stephansson, O. & Johnson, K. 1976. Granite diapirism in the Rum Jungle area, northern Australia. *Precambrian Res.* **3,** 159–185.
Talbot, C. J. 1974. Fold nappes as asymmetric mantled gneiss domes and ensialic orogeny. *Tectonophysics* **24,** 259–276.
Talbot, C. J. 1977. Inclined and asymmetric upward moving gravity structures. *Tectonophysics* **42,** 159–182.
Talbot, C. J. 1979. Fold trains in a glacier of salt in southern Iran. *J. Struct. Geol.* **1,** 5–18.
Tullis, J. & Yund, R. A. 1977. Experimental deformation of dry Westerly granite. *J. geophys. Res.* **82,** 5705–5715.
Trusheim, F. 1960. Mechanism of salt migration in Northern Germany. *Bull. Am. Ass. Petrol. Geol.* **44,** 1759.
Vidal, J. L., Kubin, L. Debat, P. & Soula, J. C. 1980. Deformation and dynamic recrystallization of K-feldspar augen in orthogneisses from Montagne Noire, Occitania, Southern France. *Lithos* **13,** 247–255.
Vitrac, A. & Allegre, C. J. 1971. Datation $^{87}Rb$-$^{87}Sr$ des gneiss du Canigou et de l'Agly (Pyrénées Orientales, France). *C. r. hebd. Séanc. Acad. Sci., Paris* **273,** 2411–2413.
Vitrac-Michard, A., Albarède, F., Depuis, C. & Taylor, H. P., Jr. 1980. The genesis of Variscan (Hercynian) plutonic rocks; inferences from Sr. Pb ad O studies on the Maladetta Igneous Complex, Central Pyrenees (Spain). *Contr. Miner. Petrol.* **72,** 57–72.
Wenk, H. R. & Wenk, E. 1969. Physical constants of alpine rocks. *Beitr. Geol. Schweiz. Kleinere Mitt.* **45,** 343.
Whitney, J. A. 1975. The effect of pressure, temperature and $XH_2O$ on phase assemblages in four synthetic rock compositions. *J. Geol.* **83,** 1–31.
Zwart, H. J. 1953. la géologie du Saint Barthélémy. *Leid. geol. Meded.* **18,** I–288.
Zwart, H. J. 1962. on the determination of polymetamorphic assemblages and its application to the Bosost area (Central Pyrenees). *Geol. Rdsch.* **52,** 38–65.
Zwart, H. J. 1965. Geological map of the Paleozoic of the Central Pyrenees. Sheet 6: Aston, France, Andorra, Spain, 1/50 000. *Leid. geol. Meded.* **33,** 191–254.
Zwart, H. J. 1968. The Paleozoic crystalline rocks of the Pyrenees in their geological setting. *Krystalinikum (Contribution to the Geology and Petrology of Crystalline complexes)*, 125–140.

Zwart, H. J. (editor) 1972. Geological map of the Pyrenees, 1/200 000. *Geological Institute, Leiden University*. Map compiled by C.R.J. Roest and H. J. Zwart.

Zwart, H. J. 1979. The geology of the Central Pyrenees. *Leid geol. Meded.* **50,** 1–74.